博士論文番号：1181204

Tight repression of yeast endoplasmic reticulum stress sensor Ire1 by its N-terminal intrinsically disordered subdomain

N 末端天然変性領域による小胞体ストレスセンサーIre1 の制御

Mathuranyanon Rubwad

Nara Institute of Science and Technology
Graduate School of Biological Sciences
Molecular and Cell Genetics Laboratory
(Assoc. Prof. Yukio Kimata)

2014/11/19

Lab Name (Supervisor)	Molecular and Cell Genetics (Assoc. Prof. Yukio Kimata)		
Name	Rubwad Mathuranyanon	Date	2014/11/19
Title	Tight repression of yeast endoplasmic reticulum stress sensor Ire1 by its N-terminal intrinsically disordered subdomain		

Abstract

In eukaryotic cells, most of secretory and transmembrane proteins are transferred to the endoplasmic reticulum (ER) for their modification and folding to the native state. Under inappropriate conditions, the ER cannot promote correct protein folding, resulting in excess unfolded proteins, which retain in the ER. There is a process called unfolded protein response (UPR) that copes with such conditions, namely ER stress. The UPR is a transcriptional activation program which induces production of a large subset of ER resident proteins, such as ER molecular chaperones and ER-associated degradation components in response to ER stress. Ire1 (Inositol-requiring enzyme 1) is an ER-located type-I transmembrane protein, which recognizes accumulation of unfolded proteins in the ER and triggers the UPR.

The luminal domain of Ire1 detects unfolded proteins accumulated in the ER and transmits the signal to its cytosolic Kinase/RNase domain, which mature the mRNA encoding the UPR-targeting transcriptional activator, Hac1. According to a recent study, the luminal domain of yeast *Saccharomyces cerevisiae* Ire1 is divided into five subdomains, namely Subregion I to V from the N-terminal to the juxtamembrane position. Subregions II to IV, called the core stress-sensing region (CSSR), form one tightly folded cavity and serve as the unfolded protein-capturing site. Another subdomain, Subregion V, is loosely folded and serves as an ER chaperone (BiP) binding site. It should be noted that under non-stress condition, BiP associates with Subregion V to inactivate Ire1, while upon ER stress, it is released from Subregion V.

In the present report, I describe a new role of another loosely folded subdomain, Subregion I, as a negative regulator of Ire1. When expressed in yeast *ire1Δ* cells, the Ire1 mutant in which Subregion I was deleted (the ΔI mutation) exhibited slightly higher activity than wild-type Ire1 under nonstress conditions. Meanwhile, wild-type Ire1 and ΔI Ire1 was almost equally activated by ER stress. Suppression of Ire1's

activity by Subregion I under nonstress conditions is likely to be physiologically important, since the ΔI mutation of Ire1 caused growth retardation of cells, although slightly. Ire1 carrying the deletion mutation of Subregion V (the ΔV mutation) was fairly activated by introduction of the ΔI mutation. This observation implies that Subregion V, to which BiP binds, and Subregion I contributes to suppression of Ire1's activity under nonstress conditions in additive manners.

We then introduced various mutations onto Subregion I of ΔV Ire1 to approach structural requirement of Subregion I for its ability to suppress Ire1's activity under nonstress conditions. Serial partial deletion of Subregion I indicated that no specific part of Subregion I is absolutely required for its ability to suppress Ire1's activity, whereas I found a 10 a.a.-long segment of the 80 a.a.-long Subregion I, namely Segment 4, which is relatively important for the Subregion-I's function. When substituted on Subregion I, intrinsically disordered peptides that are unrelated to Ire1 exhibited a Subregion-I-like function to suppress Ire1's activity. Peptides having strong ability to suppress Ire1's activity, which includes Segment 4, commonly seemed to be efficiently captured by the CSSR as its unfolded-protein substrates.

Upon ER stress, Ire1 is self-associated dependently on the CSSR to exhibit a strong activity to splice the *HAC*1 mRNA. Based on a yeast two-hybrid analysis checking homo-association of two CSSR proteins, here we propose that the CSSR is intramolecularly captures Subregion I, which inhibits self-association of Ire1. Meanwhile, under ER-stress conditions, unfolded proteins are intermolecularly captured by the CSSR, causing potent activation of Ire1. In other words, this is competition between Subregion I and unfolded proteins for association with the CSSR.

While animal or plant Ire1 orthologues do not carry N-terminal intrinsically disordered portion corresponding to Subregion I of yeast Ire1, animal PERK, which is an Ire1-family protein causing attenuation of protein synthesis upon ER stress, has it. When substituted on Subregion I of yeast Ire1, the N-terminal intrinsically disordered portion of PERK exhibited a potent ability to suppress the activity of yeast Ire1. This observation demonstrates an evolutional conservation of the negatively regulatory fashion of Ire1 and its family protein.

CONTENTS

CONTENTS (Cont.)

LIST OF FIGURES

LIST OF TABLES

LIST OF ABBREVIATIONS

BiP:	Binding Immunoglobulin Protein
bZIP:	Basic Leucine Zipper domain
DTT:	Dithiothreitol
ER:	Endoplasmic Reticulum
ERAD:	Endoplasmic Reticulum Associated Degradation
FAM:	Carboxyfluorescein-type of fluorescence dye
GGGSS:	Glycine-Glycine-Glycine-Serine-Serine amino acid residue
Hac1:	bZIP transcription factor
Hsp70:	70 kDa heat shock protein
Ire1:	Inositol-requiring enzyme 1
K_D:	Dissociation constant
*lac*Z:	β-galactosidase encoding gene
UPR:	Unfolded Protein Response
UPRE:	Unfolded Protein Response Element
RIDD:	Regulated Ire1-dependent decay
RT-PCR:	Reverse transcription polymerase chain reaction
XBP1:	X-box Binding Protein

CHAPTER I
INTRODUCTION

1.1 Endoplasmic Reticulum (ER)

The ER serves as a folding machinery for secreted and membrane proteins (Audesirk & Audesirk, 1999; Enger & Ross, 2003). Proteins produced for the cell wall, the vacuole or the other compartments of the endomembrane system first enter into the ER and are then transported to the Golgi complex *en route* to their final destination. The ER functions as a manufacturer where newly synthesized polypeptides are folded and where multi-complex proteins are assembled. Furthermore, the ER possesses a protein quality-control function, and holds the proteins until they acquire their correct conformation. These processes are performed by ER-resident soluble or membrane proteins (Vitale, *et al.*, 1993).

1.2 Protein folding and quality control in the ER

Protein folding is a process in which a polypeptide is folded to be a specific, stable, functional, correct structure. It is also a process by which proteins assembles into their functional shapes. Such a protein-folding process performed in the ER requires assistance of molecular chaperones, which facilitate folding of other proteins and avoid their aggregation and misfolding (Brodsky & Skach, 2011). Furthermore, protein folding in the ER involves various folding enzymes including protein disulfide isomerase (PDI) that facilitates formation of disulfide bonds between cysteine residues to provide structural stability of the client protein. Glycosylation (*N*-linked glycosylation) is also an important step in protein modification and folding in the ER through increasing solubility of the client proteins (Aebi, *et al.*, 2010).

The ER has a system for “proof-reading” the newly synthesized proteins, which is so-called ER quality control. Only correctly folded native proteins can reach their final destination. Meanwhile, non-native, incorrectly folded or incompletely assembled proteins are retained in the ER. Such aberrant proteins are subsequently subjected to the refolding or degradation system. Because a large number of proteins

going through the ER fail to be folded and to mature properly, cells need the ER quality-control system to be rescued from such erroneous situations.

To distinguish between correctly folded and unfolded proteins, cells use various sensor molecules including molecular chaperones, which interact specifically with misfolded or unfolded proteins. Molecular chaperones often have dual roles of assisting the folding process and of dispatching improperly folded proteins for degradation (Ellgaard & Helenius, 2003). The most abundant and best characterized ER-resident chaperone is immunoglobulin heavy chain binding protein/glucose regulated protein 78 (BiP/Grp78), which is an Hsp70 family ATPase being involved in numerous cellular functions such as translocating nascent polypeptides form cytosol to the ER, facilitating protein folding and assembly, and maintaining ER calcium homeostasis (Hendershot, 2004; Otero, *et al.*, 2010). The sensing system also involves a selective and covalent "tag" for unfolded proteins that guides the unfolded proteins to be degraded by the ER-associated degradation (ERAD) pathways. This is ubiquitin, which is a small protein that is attached to lysine side chains as a degradation signal and targets the aberrant proteins to degradation by the ubiqitin-proteasome system (Brodsky & McCracken, 1999; Glickman & Ciechanover, 2002).

Moreover, when cells are exposed to various physiological and pathological stress environments, such as glucose starvation, perturbation of calcium homeostasis, inhibition of protein glycosylation and viral infection, the ER quality control system is disturbed, leading to accumulation of misfolded or unfolded proteins. An increase of such aberrant proteins in the ER is termed ER stress and can cause severe damage of cells. However, eukaryotic cells commonly have a signal transduction feedback system, called the unfolded protein response (UPR), to cope with ER stress and maintain protein homeostasis (Gardner, *et al.*, 2013; Malhotra & Kaufman, 2007; Ron & Walter, 2007) (Fig. 1).

1.3 The Unfolded protein response (UPR)

The UPR is a cellular stress response which is conserved among all eukaryotic organisms and activated in response to the accumulation of misfolded or unfolded proteins in the ER (Ron & Walter, 2007; Taylor & Dillin, 2013). This response regulates and activates a series of adaptive mechanisms to control ER

homeostasis and to alter protein-folding status (Hetz, 2012). In other words, the UPR transmits information about the protein-folding status in the ER lumen to the nucleus and cytosol to buffer fluctuation in the unfolded protein load (Hetz, *et al.*, 2011; Schroder & Kaufman, 2005).

The UPR controls the ER-folding capacity and also partially regulates lipid biosynthesis via a transcriptional up-regulation of ER resident proteins, including ER chaperones, lipid biosynthesis proteins, and ERAD machineries. Meanwhile, the UPR also leads to a decrease in the folding load through translational repression and selective mRNA degradation (Harding, *et al.*, 1999; Hollien & Weissman, 2006; Travers, *et al.*, 2000). During severe and prolonged ER stress, the UPR induces cell death and eliminates damaged cells (Tabas & Ron, 2011; Walter & Ron, 2011).

In mammalian cells, three parallel branches of the UPR have been identified (Fig. 2). In each branch, the ER-stress sensor is ER-resident transmenbrane components, which are inositol-requiring enzyme 1 (Ire1), protein kinase RNA (PKR)-like ER kinase (PERK) and activating transcription factor 6 (ATF6). These three proteins sense misfolded or unfolded proteins accumulation in the ER lumen and transmit the information into the cytosol where a set of transcription factors carry information to the nucleus (Walter & Ron, 2011). Each branch works together to up-regulate the protein-folding activity and to decrease the number of unfolded proteins.

Ire1 is the most evolutionarily conserved ER-stress sensor, which has been found in all eukaryotes. Mammalian cells have two Ire1 paralogs, Ire1α and Ire1β, which show non-overlapping physiological roles, although these paralogs show a high degree of sequence similarity (Iwawaki, *et al.*, 2001; Tirasophon, *et al.*, 1998). Because the luminal sensor domains of PERK and Ire1 share homology, it is likely that the two proteins have similar mechanism for unfolded-protein sensing. The luminal domain of PERK transmits an unfolded-protein signal to its cytosolic kinase domain, which phosphorylates and inhibits the translational initiation factor (eIF2α). Through this pathway, PERK reduces the flux of proteins entering into the ER to alleviate ER stress. Moreover, phosphorylation of eIF2α leads to transcriptional induction of ATF4, which up-regulates downstream UPR target genes being involved in apoptosis (Bertolotti, *et al.*, 2000; Cui, *et al.*, 2011).

ATF6 is activated in response to ER stress by another different mechanism (Mori, 2003). It is constitutively synthesized as a type-II transmembrane protein in the ER. In response to ER stress, ATF6 is transported to the Golgi apparatus, where it is cleaved by the sequential action of Site-1 and Site-2 proteases (Okada, *et al.*, 2003; Shen, *et al.*, 2002; Ye, *et al.*, 2000). The cytosolic region of ATF6 is then translocated into the nucleus where it functions as a transcription activator that binds to the ER stress response element of UPR target genes (Yani & Federica, 2013).

1.4 The yeast UPR pathway and ER stress sensor Ire1

Ire1 is the ER stress sensor that has been found in all eukaryotes. It is believed that *Saccharomyces cerevisiae* (here after called yeast) does not have other ER stress sensors (Mori, 2009). Ire1 is a type-I transmembrane protein that has carboxy-terminal kinase and RNase domians on the cytoplasmic domains, while the luminal domain is likely to function to sense ER stress (Fig. 3). Under non-stress conditions, BiP is associated with and inactivates Ire1 (Fig. 4). Upon ER stress, Ire1 forms higher-order oligomers (clusters) and is auto-phosphorylated through its dissociation from BiP and direct capturing of unfolded proteins (Fig. 4; Papa, *et al.*, 2003; Gardner & Walter, 2011; Kimata, *et al.*, 2007). This event leads to full activation of the RNase domain of Ire1, which removes the intron from the substrate, *HAC*1 mRNA, via an unconventional splicing process (Cox & Walter, 1996; Sidrauski & Walter, 1997). Subsequently, the *HAC*1 mRNA exons are ligated by tRNA ligase and translated into the Hac1 protein, a basic leucine zipper transcription factor (bZIP), which induces various genes encoding factors for ER quality control to restore ER homeostasis (Travers, *et al.*, 2000; Yoshida, *et al.*, 2001).

Unlike yeast, there are two IRE1 paralogs in mammalian cells, IRE1α and IRE1β. IRE1α is ubiquitously expressed, and *IRE*1α-knockout mice are embryonic lethal, whereas IRE1β is expressed only in restricted organs and *IRE*1β-knockout mice are alive (Iwawaki, *et al.*, 2009; Tsuru, *et al.*, 2013). The IRE1-dependenent transcription factor in mammalian cells is XBP1. Similarly to Hac1, XBP1 is bZIP transcription factor and its mature mRNA is produced by an IRE1-dependent unconventional splicing in response to ER stress (Celfon, *et al.*, 2002). In addition, upon ER stress, IRE1α and IRE1β cleave and degrade mRNAs encoding secretory and

membrane proteins, leading to reduction of protein load into the ER (Hollien & Weissman, 2006).

Previous studies in my laboratory elucidated the structure of yeast Ire1 luminal domain, which comprised five subregions, namely Subregion I-V (Fig. 3) (Kimata, *et al.*, 2004; Oikawa, *et al.*, 2005). According to these studies and the crystal structure analyzed by Credle, *et al.* (2005), Subregion II to IV form a tightly folded domain, which is called the core stress-sensing region (CSSR). This domain conducts the self-association of Ire1 and forms a cavity for capturing unfolded proteins for complete activation of Ire1. Since Subregion III exists across the unfolded protein-binding cavity on the CSSR, the deletion of Subregion III abolishes the ability of CSSR to capture unfolded proteins (Phomlek, *et al.*, 2011). Subregion V, which is the BiP-binding site, is loosely folded. Since the binding of BiP on Subregion V inactivate Ire1, truncation mutations of Subregion V activate Ire1 under non-stress conditions, although slightly.

In addition to Subregion V, the luminal domain of yeast Ire1 carries another authentically disordered domain, called Subregion I, which is easily degraded by the *in vitro* proteolysis of the recombinant Ire1 proteins (Oikawa, *et al.*, 2005), at the N-terminus (Fig. 3). An Ire1 mutant carrying deletions of both Subregion I and V is constitutively self-associated, though its activity to splice the HAC1 mRNA is still regulated by ER stress (Oikawa, *et al.*, 2007). This observation implies that Subregion I might be a repressor for Ire1, function of which is independent of BiP (Oikawa, *et al.*, 2007). In my study presented here, I have addressed repression of Ire1's activity by Subregion I together with its physiological importance and mechanism.

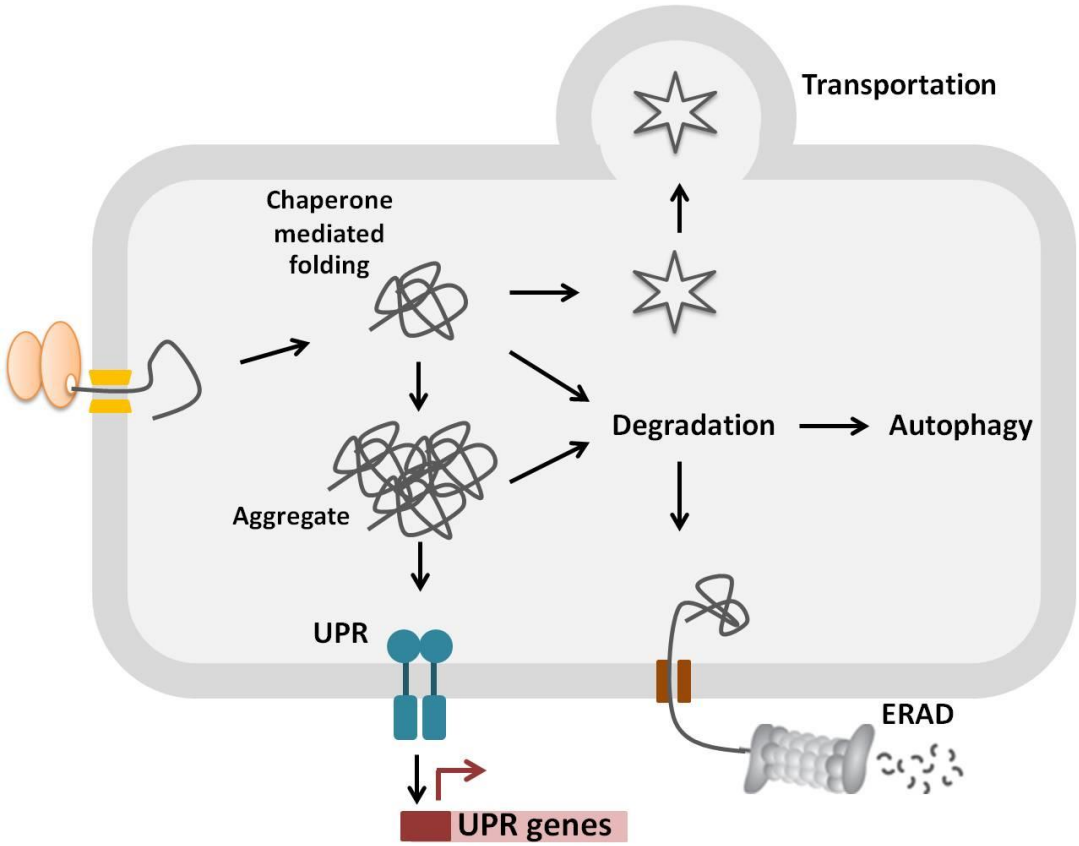

Figure 1. Protein folding and quality control in the ER. Newly synthesized polypeptides are properly folded before their transportation to the target organelles. Incorrectly folded proteins cannot exit from the ER and are degraded by the ERAD. To maintain proper protein-folding condition and prevent protein aggregation in the ER lumen, several chaperones and enzymes for glycosylation and disulfide bond formation are present in the ER. When mis-/unfolded proteins are abundant in the ER lumen, ER stress-sensor proteins recognize this aberrant situation and initiate the UPR signaling pathways.

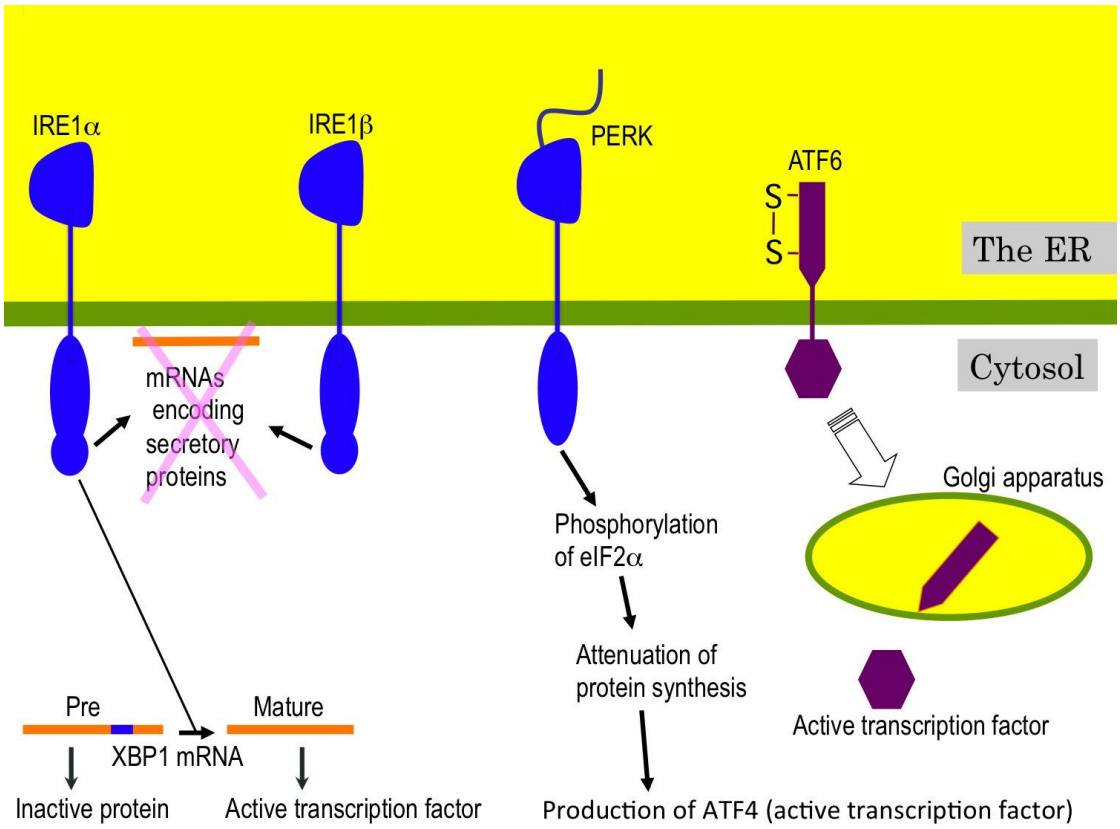

Figure 2. Three UPR signaling pathways in mammalian cells. The UPR is controlled by three ER stress sensors located on ER membrane, which recognize accumulation of unfolded proteins in the ER lumen. IRE1; Inositol-requiring kinase 1, PERK; Protein kinase RNA (PKR)-like ER Kinase, ATF6; Activating Transcription Factor 6. (Korennykn & Walter, 2012)

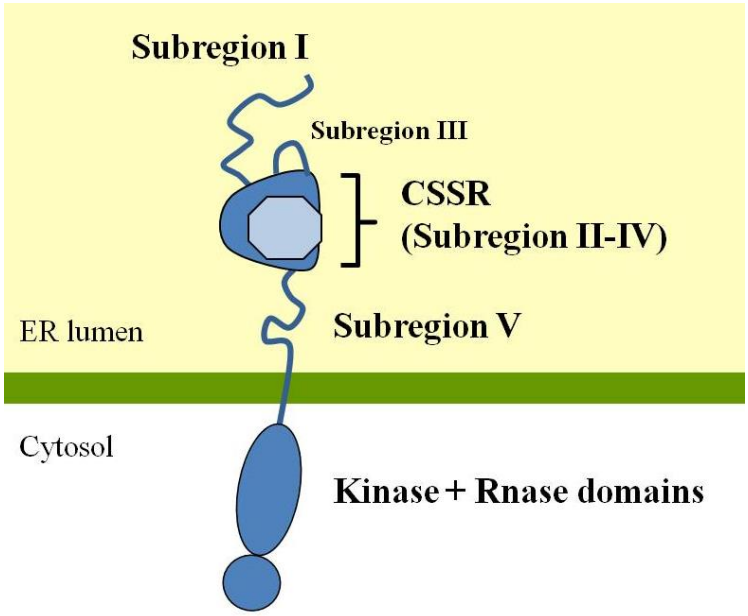

Figure 3. The structure of yeast Ire1. The luminal domain of Ire1 contains five subregions (I-V). Subregion I is disordered and located at the N-terminus of Ire1. Subregions II and IV are folded tightly and form the core stress-sensing region (CSSR). Subregion III is a loosely folded segment sticking out from the CSSR. Subregion V is loosely folded and serves as the BiP-binding site. The kinase and RNase domains are located on the cytosolic part of Ire1 (Credle, *et al.*, 2005; Kimata, *et al.*, 2004; Oikawa, *et al.*, 2005).

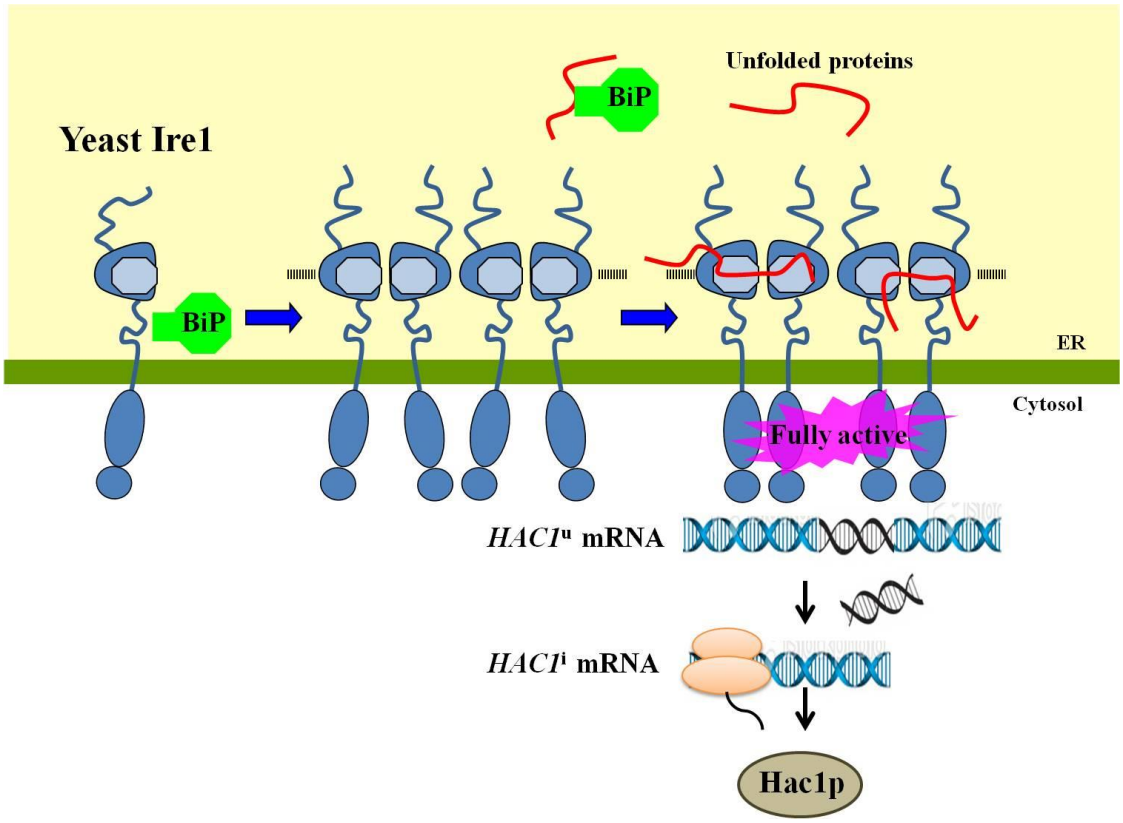

Figure 4. Yeast Ire1 signaling pathway. The type-I transmembrane protein Ire1 plays a key role in yeast UPR. Accumulation of unfolded proteins leads to release of BiP from the Ire1 luminal domain. According to Kimata *et al.* (2007), Ire1 is highly activated when unfolded proteins are recognized by the groove cavity of the CSSR, which then change the conformation on the cytosolic domain and activate the RNase domain. Activated Ire1 molecule start the unconventional splicing reaction that removes an intron from the *HAC*1 pre-mature mRNA (*HAC*1^{u} mRNA) to from the mature mRNA (*HAC*1^{i} mRNA). The *HAC*1^{i} mRNA, encoding a transcriptional activator, is translated to evoke the UPR pathway. (Gardner & Walter, 2011; Kimata, *et al.*, 2007; Promlek, *et al.*, 2011) BiP; Hsp70 family ER chaperone, *HAC*1^{u} mRNA; unspliced form, *HAC*1^{i} mRNA; spliced form, Hac1p; transcriptional factor encoding *HAC*1^{i} mRNA.

CHAPTER II
MATERIALS AND METHODS

2.1 Yeast strains and growth conditions

The two *Δire*1 strains used in this study were KMY1015 and KMY1516. KMY1015 (*MATα ura3-52 leu2-3, 112 his3-Δ200 trp1-Δ901λψσ2-801 Δire1::TRP1*) was provided by K. Mori (Kyoto University, Kyoto, Japan). This strain was mainly used for β-galactosidase activity. The β-galactosidase gene (reporter gene) was induced by the activation of wild-type and Ire1 mutants. Strain KMY1516 [(*MATα ura3-52 his3-Δ200 trp1-Δ901 LYS2::(UPRE)*$_5$*-CYC1 core promoter-lacZ::λψσ2-801 LEU2::UPRE-CYC1 core promoter-GFP::leu2-3,112 ire1::TRP1*)] was derived from KMY1015 by the insertion of UPR reporter genes [*(UPRE)*$_5$*-CYC1* core promoter-*lacZ* and *UPRE-CYC1* core promoter-*GFP*] on the chromosome. This DNA manipulation did not affect the KMY1516 phenotype under UPR activation. Both strains were grown at 30°C in minimal synthetic dextrose (SD) medium (2% glucose and 0.66% yeast nitrogen base without amino acids) supplemented with the desired amino acid according to difference in their nutrient markers and mating types.

2.2 Plasmids and generation of Ire1 mutant strains

Oligonucleotide primers used for the construction of mutant *IRE*1 plasmids are listed in Table 2.

Three plasmids carrying wild-type and mutant *IRE*1 gene used in this study were pRS313, pRS315, and pRS423. Note that pRS313 was used to express Ire1 and its mutant versions for the determination of Ire1 activity by the UPRE-*lac*Z reporter assay and *HAC*1 mRNA splicing; pRS315 was used for western blot analysis and pRS423 for immunofluorescent staining. pRS313 and pRS315 are *HIS*3- and *LEU*2-centromeric plasmids, respectively (Sikorski & Hieter, 1989). The pRS313-*IRE*1, constructed by our laboratory, was created by the insertion of *IRE*1 gene which contained its endogenous promoter at the *BamH*I/*Not*I site and carried substitutional *Sal*I and *Xba*I sites in an entire gene. To create the pRS315-*IRE*1-HA plasmid, the

introduction of a C-terminal HA-tagged sequence into the *IRE*1 gene was performed, and the obtained fragment was inserted into the *BamH*I/*Not*I site of pRS315 (Kimata, *et al.*, 2003; Okamura, *et al.*, 2000). A pRS423, the *HIS*3 2-μm plasmid, was constructed for carrying *IRE*1-HA-*Hpa*I fragment derived from *IRE*1-HA gene by replacing the *Hpa*I site on the 1.95-kbp *Sal*I–*Xba*I fragment of the *IRE*1 gene (Kimata, *et al.*, 2004). In this study, the resulting plasmid was named pRS423-*IRE*1-HA.

To generate the luminal domain mutation of Ire1, the overlap PCR method and *in vivo* gap repair techniques were performed (HO, *et al.*, 1989; Muhlrad, *et al.*, 1992). The luminal domain mutation fragments were amplified by two-step PCR to create various versions of Ire1 mutants. In the first PCR, two overlapping DNA fragments were amplified from the pRS313-ΔV *IRE*1 (Kimata, *et al.*, 2004) by the external forward primer (P1) together with the complementary deletion primers and external reverse primer (P2) together with deletion primers. Two PCR products from the first round were mixed and used as templates for the second PCR that was conducted using two other sets of primers, P3 and P4 (Table 3). The final PCR product was transformed into yeast cells by mixing the PCR product with *Sal*I/*Xba*I-digested pRS313-*IRE*1 and pRS315-*IRE*1-HA to construct pRS313 and pRS315 luminal domain mutations, respectively (Fig. 5A). To create pRS423-*IRE*1-HA mutation, the final PCR product was used together with *Hpa*I digested pRS423-*IRE*1-HA for transformation into yeast cells. All constructed plasmids were extracted from yeast cells and their sequences were confirmed by an automated 3100-*AVANT* Genetic Analyzer (Applied Biosystems, CA, USA).

The pRS313-ΔV *IRE*1 mutations that carry amino acid sequences similar to those of the yeast Subregion I from the ER stress sensor in metazoans, namely PERK, were constructed. The 56-a.a. of human and mouse PERK N-termini were amplified using a set of *Spe*I-franking forward and *Mlu*I-franking reverse primers listed in Table 2. Plasmid pTKbasal-hPERK-HA WT (constructed by our laboratory) and pCDNA1-mPERK-myc [provided by D.Ron (Harding, *et al.*, 1999)] were used as PCR templates for human and mouse PERK, respectively. Subsequently, the PCR products were inserted into *Spe*I and *Mul*I sites of pRS313-ΔV *IRE*1 which was modified to carry the *Spe*I and *Mul*I sites on the luminal domain of *IRE*1 gene, as showed in Figure 5C. Finally, human and mouse PERK N-termini were substituted on the first 60-a.a.

residue of yeast Subregion I in pRS313-ΔV *IRE*1 (denoted as pRS313-hPREK-ΔV *IRE*1 and pRS313-mPERK-ΔV *IRE*1, respectively). To introduce N-terminal sequences from human and mouse PERK into pRS315-ΔV *IRE*1-HA and pRS423-ΔV *IRE*1-HA, P3 and P4 primers were used to amplified DNA fragments carry mutant *IRE*1 using pRS313-hPREK-ΔV *IRE*1 and pRS313-mPERK-ΔV *IRE*1 as templates. These PCR products were introduced into each pRS315-ΔV *IRE*1-HA and pRS423-ΔV *IRE*1-HA by in vivo gap repair techniques as described above.

The 56-a.a. sequences of Subregion I from another fungus Ire1 (*Aspergillus oryzae*) and the disordered sequences from other proteins (San1 and TOPII) were replaced on the first 60-a.a. of yeast Subregion I in pRS313-ΔV *IRE*1 using the same methodology as that for pRS313-hPREK-ΔV *IRE*1 (also for pRS315-ΔV *IRE*1-HA and pRS423-ΔV *IRE*1-HA) (Table 4). San1 and TOPII are *Saccharomyces cerevisiae* proteins that function as nuclear ubiquitin ligase and Topoisomerase enzymes, respectively (Berger, *et al.*, 1996; Rosenbaum, *et al.*, 2011). Both proteins carry disordered residues in an entire sequence.

The plasmids that carry DNA sequences encoding for six tandem repeats of the GlyGlyGlySerSer residue [here after denoted as $(GGGSS)_6$] and three tandem repeats of the segment 4th of Subregion I [hereafter denoted as $(segment4)_3$] were chemically synthesized by TAKARA BIO Inc., (Japan). These DNA fragments were flanked by 5'- *Spe*I and 3'- *Mlu*I sequences. Each fragment was cut from synthetic plasmids and inserted into *Spe*I and *Mlu*I sites of modified pRS313-ΔV *IRE*1 to create pRS313-$(GGGSS)_6$ΔV *IRE*1 or pRS313-$(segment4)_3$ΔV *IRE*1 plasmids (Fig. 5B).

The pCZY1 is a yeast 2-μm plasmid carrying the *URA*3 selectable marker and *E.coli lacZ* reporter gene (Mori, *et al.*, 1992). This plasmid was used to determine the activity of UPR-activated IRE1 in yeast cells because *lacZ* gene in pCZY1 plasmid is under the control of a promoter element of *HAC*1 gene (UPR element) and is up-regulated by UPR.

For the construction of the mNeonGreen-tagged version of Ire1 and the mutant, *IRE1*-encoding gene was fused to the mNeonGreen sequence and inserted into pRS313 plasmid. See Aragon *et al*., (2009) for the insertion position of the *IRE1* gene.

A.

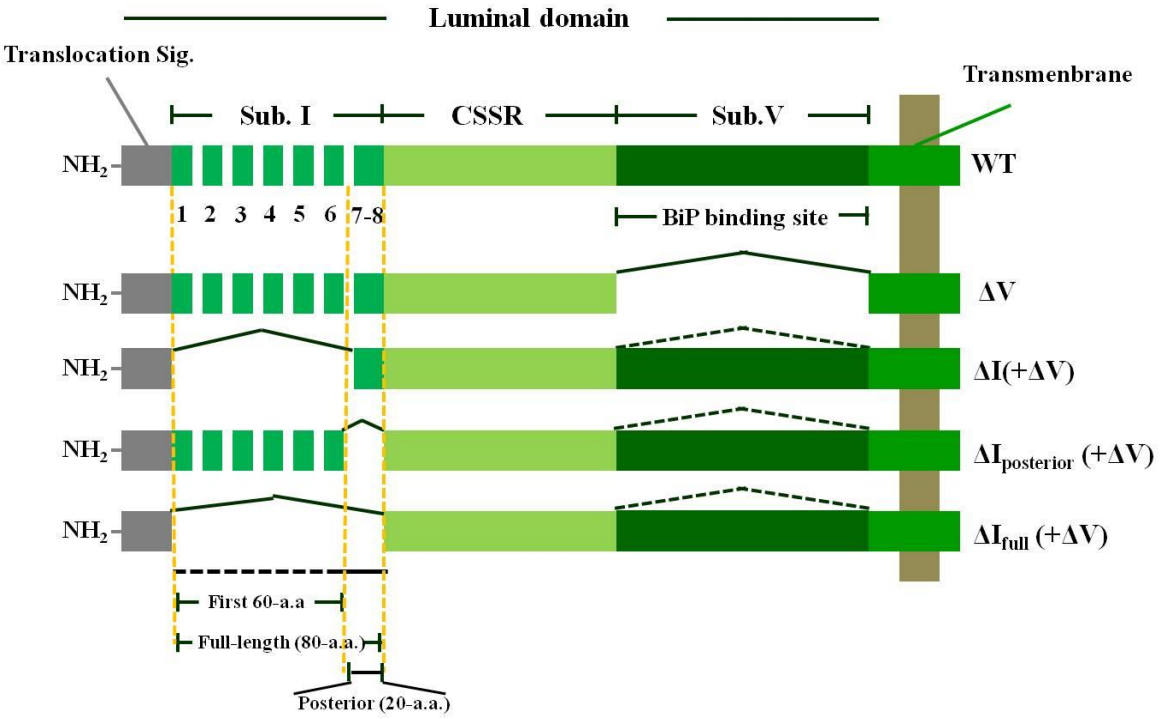
Luminal domain
Translocation Sig.
Transmenbrane
Sub. I
CSSR
Sub.V
NH2
WT
1 2 3 4 5 6 7-8
BiP binding site
ΔV
ΔI(+ΔV)
ΔIposterior (+ΔV)
ΔIfull (+ΔV)
First 60-a.a
Full-length (80-a.a.)
Posterior (20-a.a.)

B.

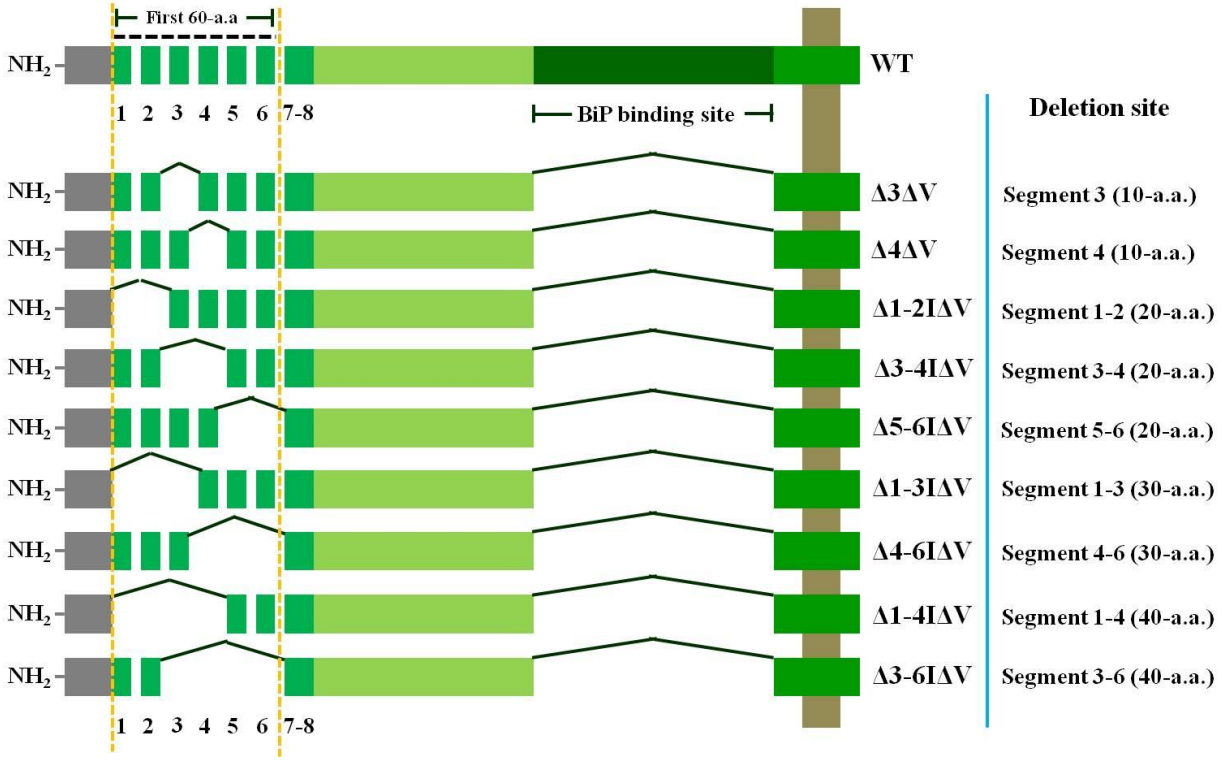
First 60-a.a
NH2
WT
1 2 3 4 5 6 7-8
BiP binding site
Deletion site
Δ3ΔV
Segment 3 (10-a.a.)
Δ4ΔV
Segment 4 (10-a.a.)
Δ1-2IΔV
Segment 1-2 (20-a.a.)
Δ3-4IΔV
Segment 3-4 (20-a.a.)
Δ5-6IΔV
Segment 5-6 (20-a.a.)
Δ1-3IΔV
Segment 1-3 (30-a.a.)
Δ4-6IΔV
Segment 4-6 (30-a.a.)
Δ1-4IΔV
Segment 1-4 (40-a.a.)
Δ3-6IΔV
Segment 3-6 (40-a.a.)

C.

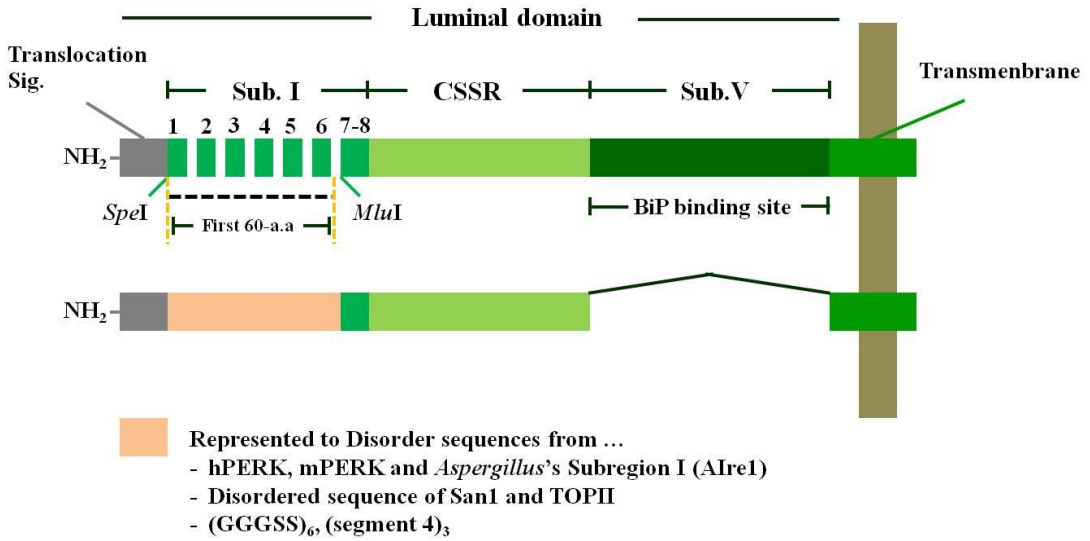

Figure 5. The scheme of luminal domain of wild-type Ire1 (WT) and luminal domain mutants. (A.) Single deletion of Subregion I mutants and double deletion of Subregion I together with Subregion V (dashed line). (B.) The partial deletion of luminal domain mutants. (C.) The luminal domain mutant carried the N-terminal sequence of humanPERK, mousePERK. *A. oryzae* Ire1, disordered sequence of San1 and TOPII and tandem repeat of GGGSS or tandem repeat of segment 4 sequences.

2.3 Yeast transformation

Yeast cells were inoculated into 1 mL of yeast peptone dextrose (YPD) medium and overnight cultured at 30°C. Then, all cells were transferred to 50 mL of fresh YPD medium in 300 mL flasks and incubated for approximately 4-5 h (mid-logarithmic phase). Cultured cells were collected by centrifugation at 3,000 rpm for 2 min and suspended with 10 mL of 0.1 M LiAc/TE solution. After centrifugation, the supernatant was removed, and cells were dissolved with 1 mL LiAc/TE solution followed by incubation at 30°C with shaking at 60 rpm for 60 min. One hundred microliters of cells were transferred into 1.5-mL microtubes that contained 5 µL of carried DNA and 1 µg of transforming DNA. The mixed solution was incubated at 30°C for 30 min. Then 800 µL of 40% Polyethylene Glycol 4000 was added to the mixture. The transformation mixture was further incubated at 30°C for 1 h and then 100 µL of the mixture was spread on Synthetic define (SD) medium supplemented with appropriate amino acid. Cells were incubated at 30°C for 2-3 days.

2.4 β-galactosidase assay

Overnight cultures were inoculated into a fresh medium and further incubated at 30°C with shaking until cells reached the logarithmic phase. Cells were collected by centrifugation at 10,000 rpm for 2 min and suspended with 800 µL of Z buffer (60 mM Na_2HPO_4, 40 mM NaH_2PO_4, 10 mM KCl, 1 mM $MgSO_4$, and 0.27% of 2-mercaptoethanol, pH 7.0). Fifty microliters of chloroform and 20 µL of 0.1% SDS were added to the suspended cells and then vigorously mixed for 20 sec. The mixture was incubated at 28°C for 5 min. The *o*-Nitrophebyl-β-D-galactoside (4 mg/mL in Z buffer), which is a β-galactosidase substrate, was added to the mixture at final concentration of 0.8 mg/mL and further incubated at 28°C until the color of the mixture changed to pale yellow. The reaction was stopped by 500 µL of 1 M $NaCO_3$. The concentration of *o*-nitro-phenol (ONP), the final product, was measured using a spectrophotometer at a wavelength of 420 nm. Reaction definition was examined as one unit of β-galactosidase activity for the production of 1 nmol of ONP per minute of reaction for 1 mL of cultured cells at 1 DO_{600}. The β-galactosidase activity could be calculated as follows.

$$6\ \ \beta\text{-galactosidase activity} = \frac{OD_{420}\times 375}{OD_{600}\times \text{time (min)}}$$

2.5 Fluorescent-tagging and localization of Ire1

A wild-type or ΔIΔV Ire1-mNeonGreen-tagged molecule was visualized by fluorescent image processing using the Delta Vision Elite microscopy system (Applied Precision) with the GFP excitation/emission filter set. For the observation of the Ire1 HA-tagged protein, cells fixing and experimental protocols were described in (Kimata, *et al.*, 2007). The stained cells were visualized under a fluorescent microscope (Axiophoto, Carl Zeiss Microimaging), and images were taken by a digital charge-coupled device camera system (DP70, Olympus).

2.6 *HAC*1 mRNA splicing

2.6.1 RNA preparation

Total RNA preparation was performed by the hot phenol method (Kimata, *et al.*, 2004). Cells, at approximately OD600 = 1 were harvested and resuspended with 400 µL of buffer (50 mM NaAC (pH 5.3) and 10 mM EDTA). Then, 40 µL of 10% SDS was added followed by 400 µL of water-saturated hot phenol, which was incubated at 65°C before use, and gentle mixed for 30 sec. The suspension was incubated at 65°C for 1 h coupled with 30 sec maximum speed mixing for three times. Subsequently, the suspension was chilled at -80°C for 90 min and thawed at room temperature. The thawed mixture was centrifuged at 13,000 rpm for 10 min at room temperature, and the water fraction was collected into a new tube. Two phenol-chloroform extractions were performed, and RNA was precipitated by 1/10 volume of 3 M NaAC (pH 5.3) and 2.5 volumes of absolute ethanol. RNA was washed by 70% ethanol and dried. Finally, the pellet of RNA was dissolved in water and stored at -80°C.

2.6.2 Reverse transcription (RT)-PCR assay

One microgram of total RNA was conversed to cDNA by the Superscript^{TM}II Reverse Transcriptase (Invitrogen) and oligo (dT) primers with sequences according to the manufacturer's protocol. For the amplification of *HAC*1^{u} and *HAC*1^{i}, 2 µL of

cDNA was added to a total of 25 µL of reaction mixture containing 1 µL of 10 µM *HAC*1 primers (Table 3), 1X PCR buffer, 2 µL of 2.5 mM dNTP and 0.13 µL of KAPA taq DNA polymerase (5 U/µL) (Kapa Biosystem). The amplification condition was denaturation at 96°C for 5 min followed by 25 cycles of amplification with denaturation at 94ºC for 30 sec, annealing at 54ºC for 30 sec, and extension at 72ºC for 1 min. An extra extension step of 7 min at 72ºC was carried out after the completion of amplification for 25 cycles. The PCR products were analyzed by agarose gel electrophoresis, and the fluorescent images were captured by LAS-4000 camera (Fujifilm, Japan). The intensity of *HAC*1^{i} and *HAC*1^{u} fragments were quantified by the Fujifilm Image Gauge software. The percentage of *HAC*1 mRNA splicing was calculated according the following formula.

$$\%\ HAC1\ \text{mRNA splicing} = \frac{HAC1^{i}}{HAC1^{i} + HAC1^{u}} \times 100$$

2.7 Western blot analysis

2.7.1 Preparation of protein samples

Yeast cells were grown on SD medium supplemented with desired amino acid at 30°C with shaking. Approximately five OD_{600} equivalents of cells were harvested and re-suspended with 100 µL of lysis buffer (50 mM Tris-HCl pH 7.9, 5 mM EDTA and 1% Triton X-100) and protease inhibitors (2 mM phenylmethanesulfonyl fluoride, 1/100 volume of protease inhibitor cocktail set III (EDTA-free) and 10 µg/L of pepstain, leupeptin and aprotinin). Cells in the mixture solution were lysed by mechanical force using 0.5-mm glass beads with hi-speed vortex for 30 sec repeated 6 times. Protein extract was collected by centrifugation at 10,000 rpm, 4°C for 10 min and stored at -80°C.

2.7.2 Electrophoresis and protein detection

Ten micrograms of protein sample were denatured in SDS/DTT buffer and subjected to 10% SDS-acrylamide gel electrophoresis. Proteins were transferred onto immobilon-P transfer membrane (Millipore, USA) at 1 mA/cm^2 for 90 min. The transferred proteins were blocked by incubation with a buffer containing 5% skim

milk in 0.2% Tween 20/PBS (0.2% PBST) at room temperature for 1 h or at 4°C overnight. After indicated times, proteins were probed with 1:4000 dilution of primary anti-bodies [12CA5 anti-HA mouse IgG (Roche Applied Science)] in 5% skim milk with 0.2% PBST at room temperature for 1 h, and then the membrane was washed with 0.2% PBST for 5 min three times. The secondary anti-body (1:4000 dilution of HRP-conjugated goat anti-mouse IgG) was diluted in 5% skim milk with 0.2% PBST. One hour incubation at room temperature was performed followed by membrane washing with 0.2% PBST for 5 min three times. The indicated protein band was detected by developing with solution activated chemiluminescence, ECL Western blotting detection system (GE Healthcare, UK). ECL signals were then detected by X-ray film exposure.

2.8 Yeast Two Hybrid assay

2.8.1 Yeast strains and growth condition

The host strain carrying the *GAL*4 DNA binding domain (BD) fusd to bait proteins was Y2HGold (*MATa*, *trp*1-901, *leu*2-3, 112, *ura*3-52, *his*3-200, *gal*4Δ, *gal*80Δ, *LYS*2::*GAL*1$_{UAS}$-*Gal*1$_{TATA}$-*His*3, *GAL*2$_{UAS}$-*Gal*2$_{TATA}$-*Ade*2 *URA*3::*MEL*1$_{UAS}$-*Mel*1$_{TATA}$-*AUR*1-C *MEL*1). This strain has *AbA*^{r}, *HIS*3, *ADE*2, and *MEL*1 as reporter genes. Strain 187 (*MATα*, *ura*3-52, *his*3-200, *ade*2-101, *trp*1-901, *leu*2-3, 112, *gal*4 *gal*4Δ, *gal*80Δ, *met-URA*3::*GAL*1$_{UAS}$-*Gal*1$_{TATA}$-*LacZ*, *MEL*1) was a *GAL*4 activation domain (AD) fused to prey protein carriers containing *MEL*1 and *lacZ* reporter genes (Harper, *et al.*, 1993). Both strains were grown at 30°C on YPD medium supplemented with adenine (YPDA, 2% glucose, 1% yeast extract, 2% peptone and 0.01% adenine hemisulfate).

2.8.2 Plasmids

To generate all bait protein plasmids, the oligonucleotide was inserted in frame with *GAL*4 DNA-BD at appropriate restriction endoribonuclease sites of the *Kan*^{r}-pGBKT7 plasmid (Clontech Laboratory Inc., CA), according to the primers used. Almost all oligonucleotides were single amplified using DNA templates and primers listed in Table 5. However, the construction of five plasmids, listed in Table 5, was different [denoted as pGBK-(1-3)$_2$I, pGBK-(4-6)$_2$I and pGBK-(Segment4)$_6$, pGBK-

$(GGGSS)_{12}$, and pGBK-$(TopII)_2$]. These repeated nucleotides were double amplified using two different sets of primers that produced two PCR products. The resulting first PCR fragment was flanked by 5'*EcoR*I and 3'*Cla*I sites at each end, and the second PCR fragment was flanked by 5'*Cla*I and 3'*BamH*I at each end. Two nucleotides were joined together at the *Cla*I site and inserted into *EcoR*I and *BamH*I sites of pGBKT7 plasmid. All bait plasmids were transformed into the Y2HGold strain.

The plasmids carrying the *GAL*4 AD-fused prey protein were constructed by the in-frame insertion of prey oligonucletides into the indicated site of the Amp^r-pGADT7 plasmid (Clontech Laboratories Inc., CA) according to the primer used (Table 5). All types of pGADT7 plasmids were transformed into the 187 strain.

2.8.3 Two-Hybrids assay

Y2HGold and 187 strains carrying bait and prey plasmids, respectively, were co-cultured in 2xYPDA medium. Culture condition is described in Matchmaker™ Gold Yeast Two-Hybrid System manufacturer's instructions (Clontech Laboratories Inc., CA). The co-cultured cells were then diluted and dropped on double dropout (DDO/A) (-leucine and -tryptophan) or triple dropout (TDO/A) (-leucine, -tryptophan and -histidine) media, containing 125 ng/mL Aureobasidin A (1% glucose, 0.33% yeast nitrogen base w/o amino acid, 1% agar and an appropriate amount of essential amino acids except leucine, tryptophan, or histidine) (Folter & Immink, 2011), incubated at 30°C for 3-4 days.

2.9 Fluorescence Anisotropy

The Ire1 CSSR was expressed in *E. coli* and purified as described by Kimata (2007). However, we changed the percentage of glycerol in the elution buffer to 10% final concentration. The synthetic FAM-labeled peptide (ΔEspP-FAM), which was according to Gardner and Walter (2011), was purchased from GL Biochem (Shanghai, China). All short un-labeled peptides derived from segment 2, 3, 4, 5 and 6 of Subregion I (Table 1) were synthesized by Sigma-Aldrich (MO, USA).

Table 1. Amino acid sequence of un-labeled peptides

Peptide	**Amino acid sequence**
Segment 2	KKKAVASTKKLNFNAAKKKK
Segment 3	KKKAYGVDKNINSPAAKKKK
Segment 4	KKKAIPAPRTTEGLAAKKKK
Segment 5	KKKAPNMKLSSYPTAAKKKK
Segment 6	KKKAPNLLNTADNRAAKKKK

- The 10 underlined amino acids represent each segment.

The binding of Ire1 CSSR to ΔEspP-FAM was analyzed by comparing the change in fluorescence anisotropy according to the concentration of Ire1 CSSR. The fluorescence polarization reader was the single tube Beacon^{TM} 2000 (Invitrogen, USA), and it required a controlling temperature of 25°C and the reaction volume of 100 μL in each single tube. The purified Ire1 CSSR was mixed with constant 10 μM of ΔEspP-FAM in the microtube and incubated at room temperature for 30 min. Buffers used in the assay were 50 mM Hepes, 100 mM KCl, 5 mM MgCl2, 200 mM Imidazole, and 10% (v/v) glycerol, same as the elution buffer used in the protein purification method. Then fluorescence polarization value was measured and calculated to the anisotropy value as follows; $(I_{II} - I_{\underline{I}}) / (I_{II}+2I_{\underline{I}})$; here I_{II} is the intensity of emitted light polarized parallel to the excitation light, and $I_{\underline{I}}$ is the intensity of emitted light polarized perpendicular to the excitation light. The K_D was estimated from the graph of the plot between anisotropy value and concentration of Ire1 CSSR (μM) and was used for the competitive interaction assay.

To analyze the affinity binding of each segment (2 to 6), we used the un-labeled peptides (Table 1) as competitors in the binding reaction of Ire1 CSSR to ΔEspP-FAM. Various concentrations of each un-labeled peptide were added to the mixture of constant 5 μM of Ire1 CSSR and 10 μM of ΔEspP-FAM and incubated at room temperature for 45 min. Anisotropy values were plotted according to the concentration of each un-labeled peptide. The decrease in anisotropy values depends on the affinity binding of each competitor segment to the Ire1 CSSR domain.

Table 2. Primers for the construction of plasmids carrying mutant *IRE*1 gene

Mutant	Primer name	Primer sequence	Template
ΔI(+ΔV)	ΔI F[d]	5’ TGCTCAATCCCATTGTCGTCTCGCCGTGCTAACAAAAAAGGACGTAGG 3’	pRS313 *IRE*1 or pRS313 ΔV *IRE*1 (Kimata, *et al.*, 2004)
	ΔI R[c]	5’ CCTACGTCCTTTTTTGTTAGCACGGCGAGACGACAATGGGATTGAGCA 3’	
$\Delta I_{posterior}$ (+ΔV)	$\Delta I_{posterior}$ F[d]	5’ TTATTGAATACTGCTGATAATCGACGTTCCTTGAACGAACTGAGTTTA 3’	
	$\Delta I_{posterior}$ R[c]	5’ TAAACTCAGTTCGTTCAAGGAACGTCGATTATCAGCAGTATTCAATAA 3’	
ΔI_{full}(+ΔV)	ΔI_{full} F[d]	5’ TGCTCAATCCCATTGTCGTCTCGCCGTTCCTTGAACGAACTGAGTTTA 3’	
	ΔI_{full} R[c]	5’ TAAACTCAGTTCGTTCAAGGAACGGCGAGACGACAATGGGATTGAGCA 3’	
Δ1-4IΔV	Δ1-4I F[d]	5’ TGCTCAATCCCATTGTCGTCTCGCCCAAATATGAAACTCAGCTCATAT 3’	pRS313 ΔV *IRE*1
	Δ1-4I R[c]	5’ ATATGAGCTGAGTTTCATATTTGGGCGAGACGACAATGGGATTGAGCA 3’	
Δ3-6IΔV	Δ3-6I F[d]	5’ TCCACTAAAAAGCTCAATTTCAACCGTGCTAACAAAAAAGGACGTAGG 3’	
	Δ3-6I R[c]	5’ CCTACGTCCTTTTTTGTTAGCACGGTTGAAATTGAGCTTTTTAGTGGA 3’	
Δ1-3IΔV	Δ1-3I F[d]	5’ TGCTCAATCCCATTGTCGTCTCGCATTCCTGCTCCAAGAACCACTGAA 3’	
	Δ1-3I R[c]	5’ TTCAGTGGTTCTTGGAGCAGGAATGCGAGACGACAATGGGATTGAGCA 3’	
Δ4-6IΔV	Δ4-6I F[d]	5’ GTGGATAAAAATATAAACTCGCCCCGTGCTAACAAAAAAGGACGTAGG 3’	
	Δ4-6I R[c]	5’ CCTACGTCCTTTTTTGTTAGCACGGGGCGAGTTTATATTTTTATCCAC 3’	
Δ1-2IΔV	Δ1-2 F[d]	5’ TGCTCAATCCCATTGTCGTCTCGCTATGGTGTGGATAAAAATATAAAC 3’	
	Δ1-2 R[c]	5’ GTTTATATTTTTATCCACACCATAGCGAGACGACAATGGGATTGAGCA 3’	

Table 2. Primers for the construction of plasmids carrying mutant *IRE*1 gene (Continued)

Mutant	Primer name	Primer sequence	Template
Δ3-4IΔV	Δ3-4I F[d]	5’ TCCACTAAAAAGCTCAATTTCAACCCAAATATGAAACTCAGCTCATAT 3’	pRS313 ΔV *IRE*1
	Δ3-4I R[c]	5’ ATATGAGCTGAGTTTCATATTTGGGTTGAAATTGAGCTTTTTAGTGGA 3'	
Δ5-6IΔV	Δ5-6I F[d]	5’ ATGAAACTCAGCTCATATCCAACTAATTCTATAAGTGTACCCTATTTG 3’	
	Δ5-6I R[c]	5’ CAAATAGGGTACACTTATAGAATTAGTTGGATATGAGCTGAGTTTCAT 3’	
Δ3IΔV	Δ3I F[d]	5’ TCCACTAAAAAGCTCAATTTCAACATTCCTGCTCCAAGAACCACTGAA 3’	
	Δ3I R[c]	5’ TTCAGTGGTTCTTGGAGCAGGAATGTTGAAATTGAGCTTTTTAGTGGA 3’	
Δ4IΔV	Δ4I F[d]	5’ GTGGATAAAAATATAAACTCGCCCCCAAATATGAAACTCAGCTCATAT 3’	
	Δ4I R[c]	5’ ATATGAGCTGAGTTTCATATTTGGGGGCGAGTTTATATTTTTATCCAC 3’	

- The letter d and c indicated deletion and complementary deletion primers, respectively.

Table 3. External deletion primers and primer for *HAC*1 mRNA splicing

	Primer name	Primer sequence
External primers	P1	5’ GAGATTAATCACATAGTAACAAGAA 3’
	P2	5’ TCAGGTTTTCATCTGATACATTCTT 3’
	P3	5’ CCATTATCACTTTTCTCCATATCA 3’
	P4	5’ CCTTGAAAACTTCCCTGAAAAACT 3’
RT-PCR	Hac1 F	5’ TACAGGGATTTCCAGAGCACG 3’
	Hac1 R	5’ TGAAGTGATGAAGAAATCATTCAATTC 3’

Table 4. Primers for the construction of plasmids carrying chimeric *IRE*1 mutant

Mutant	Primer name	Primer sequence	Template
hPREK-ΔV *IRE*1	Spe-hPERK1 F	5’ GGACTAGT[1]GGGCGCGCCCGTGGCCTC 3’	pTKbasal-hPERK-HA WT
	Mlu-hPERK2 R	5’ CGACGCGT[2]CGCGGCTGCCGGCAGCGC 3’	
mPREK-ΔV *IRE*1	Spe-mPERK1 F	5’ GGACTAGT[1]GTCGCGCCCGCCCGCAGT 3’	pCDNA1-mPERK myc
	Mlu-mPERK2 R	5’ CGACGCGT[2]TTCGCCAGCGGCAGCCGG 3’	
AIre1-ΔV *IRE*1	Spe-AIre 1 F	5’ GGACTAGT[1]CAGCAGCAGCCGGAACAT 3’	Genomic DNA of *Aspergillus oryzae*
	Mlu-AIre 2 R	5’ CGACGCGT[2]GCGGCCGGGGCCCGCCAG 3’	
San1-ΔV *IRE*1	Spe-SC	5’ GGACTAGT[1]GTTCCCACTATCGGAAAT 3’	Genomic DNA of *S. cerevisiae*
	Mlu-SC	5’ CGACGCGT[2]GGGTGGATTTTGAGTAGT 3’	
TopII-ΔV *IRE*1	Spe-TOPII	5’ ACTAGT[1]GATAAAGATTACATT 3’	Genomic DNA of *S. cerevisiae*
	Mlu-TOPII	5’ ACGCGT[2]AGGTTCGTATTGTCT 3’	

- Underlined nucleotides indicate [1]*Spe*I and [2]*Mlu*I sites, respectively.

Table 5. Plasmids and primers for Yeast Two Hybrid assay

- Construction of pGBKT7 carrying the bait protein.

Plasmid name	Primer name	Primer sequence	Template	Insertion sites
pGBK-I-CSSR	Forward; *Nco*I-I	5’ GGCCATGG[3]ATGTCAAGGCGGCAGATAGTG 3’	pRS313 *IRE*1 WT	*Nco*I/ *BamH*I
pGBK-I-ΔIIICSSR			pRE315 *IRE*1-HA* ΔIII	
pGBK-I-MFY CSSR	Reverse; pGBK-CoreR	5’ CGGGATCC[4]ATCATATTCATTATTATA 3’	pRE315 *IRE*1-HA* Groove mutant	
pGBK-CSSR	*Nco*I-Core	5’ GGCCATGG[3]ATGTCCTTGAACGAACTGAGT 3’	pRS313 *IRE*1 WT	
	pGBK-CoreR	5’ CGGGATCC[4]ATCATATTCATTATTATA 3’		
pGBK-SubI	pGBK-I(A)F	5’ CCGAATTC[5]ATGTCAAGGCGGCAGATAGTGGAA 3’	pRS313 *IRE*1 WT	*Eco*RI/ *BamH*I
	pGBK-I(A)R	5’ ACGGATCC[4]TCGATTATCAGCAGTATTCAATAA 3’		
pGBK-hPERK	Eco-hPERK	5’ CGGAATTC[5]ATGGGGCGCGCCCGTGGC 3’	pTKbasal-hPERK-HA WT	
	Bam-hPERK	5’ CGGGATCC[4]ACCCCGAGGCTCCTGCTC 3’		
pGBK-mPERK	Eco-mPERK	5’ CGGAATTC[5]ATGGTCGCGCCCGCCCGC 3’	pCDNA1-mPERK myc	
	Bam-mPERK	5’ CGGGATCC[4]CTCCGTCGCGCGTGACTC 3’		

Table 5. Plasmids and primers for Yeast Two Hybrid assay

- Construction of pGBKT7 carrying the bait protein. (Continued)

Plasmid name	Primer name		Primer sequence	Template	Insertion sites
pGBK-San1	Eco-San1		5’ CGGAATTC[5]ATGGTTCCCACTATCGGA 3’	pRS313-San1-ΔV *IRE*1	*EcoR*I/ *BamH*I
	Bam-San1		5’ CGGGATCC[4]AGAATTAGAGGGTGGATT 3’		
pGBK-(segment4)$_6$	1st PCR	Eco-Re4	5’ CGGAATTC[5]ATGATTCCTGCTCCAAGA 3’	pRS313-(segment4)$_3$ ΔV *IRE*1	
		Cla-Re4 R	5’ CCATCGATT[6]AGACCTTCTGTGGT 3’		
	2nd PCR	Cla-Re4 F	5’ CCATCGATA[6]TTCCTGCTCCAAGA 3’		
		Bam-Re4	5’ CGGGATCC[4]TGTGGTTCTTGGAGC 3’		
pGBK-(GGGSS)$_{12}$	1st PCR	Eco-GS	5’ CGGAATTC[3]ATGTCAGGTGGAGGAAGTTCA 3’	pRS313-(GGGSS)$_6$ ΔV *IRE*1	
		Cla-GS R	5’ CCATCGAT[6]ACCACCACTTGAACCTCC 3’		
	2nd PCR	Cla-GS F	5’ CCATCGAT[6]GGAGGTGGAGGAAGTTCA 3’		
		Bam-GS	5’ CGGGATCC[4]ACCTCCACCACTTGAACCTCC 3’		
pGBK-(1-3)$_2$I	1st PCR	Eco-13I	5’ GAATTCAT[5]GACCTCAAGGCGGCAGAT 3’	pRS313 *IRE*1 WT	
		Cla-13I R	5’ TATCGAT[6]GGGCGAGTTTATATTTT 3’		
	2nd PCR	Cla-13I F	5’ ATCGAT[6]ACCTCAAGGCGGCAGATA 3’		
		Bam-13I	5’ GGATCCG[4]GGCGAGTTTATATTTTT 3’		

Table 5. Plasmids and primers for Yeast Ywo Hybrid assay

- Construction of pGBKT7 carrying the bait protein. (Continued)

Plasmid name	Primer name		Primer sequence	Template	Insertion sites
pGBK-(4-6)$_2$I	1st PCR	Eco-46I	5’ GAATTC[5]ATGATTCCTGCTCCAAGAAC 3’	pRS313 *IRE*1 WT	*EcoR*I/ *BamH*I
		Cla-46I R	5’ ATCGAT[6]TCGATTATCAGCAGTATT 3’		
	2nd PCR	Cla-46I F	5’ ATCGAT[6]ATTCCTGCTCCAAGAACC 3’		
		Bam-46I	5’ GGATCC[4]TCGATTATCAGCAGTATTC 3’		
pGBK-(TopII)$_2$	1st PCR	Eco-TOPII	5’ GAATTC[5]ATGGATAAAGATTACATTGA 3’	pRS313 *IRE*1 WT	
		Cla-TOPII	5’ ATCGAT[6]AGGTTCGTATTGTCTCAG 3’		
	2nd PCR	Cla-TOPII	5’ ATCGAT[6]GATAAAGATTACATTGAT 3’		
		Bam-TOPII	5’ GGATCC[4]AGGTTCGTATTGTCTCAG 3		

- Underlined nucleotides indicate [3]*Nco*I, [4]*BamH*I, [5]*EcoR*I, and [6]*Cla*I sites.

Table 5. Plasmids and primers for Yeast two hybrid assay

- For construction of pGADT7 carrying the prey protein.

Plasmid name	Primer name	Primer sequence	Template	Insertion sites
pGAD-CSSR	Forward; *BamH*I-Core	5’ CG<u>GGATCC</u>[4]ATGCGTTCCTTGAACGAA 3’	pRS313 *IRE*1 WT	*BamHI*/ *Xho*I
pGAD-ΔIII CSSR				
pGAD-MFY CSSR	Reversed; *Xho*I-Core	5’ CC<u>CTCGAG</u>[7]TTAATCATATTCATTATT 3’		

- Underlined nucleotides indicate [4]*BamH*I and [7]*Xho*I sites.

CHAPTER III
RESULTS

3.1 Subregion I is intrinsically disordered

As described in the Introduction section, Kimata *et al.* (2004) and Oikawa, *et al*. (2005) mapped the luminal domain of yeast Ire1. The amino acid (a.a.) residues 1-31 work as the ER-translocation signal sequence and thus are probably removed co-translationally. Subregion I, which corresponds to a.a. position 32-111, is thus located at the N-terminus of Ire1. It is sequentially connected with the CSSR containing Subregion II (a.a. 112-242), Subregion III (a.a. 243-272), and Subregion IV (a.a. 273-454), and Subregion V (a.a. 455-524) (Fig. 3 and 5). Although a number of previous reports touched on structure and function of the CSSR and Subregion V, to my knowledge, there has been no study approaching those of Subregion I.

The predictor of naturally disordered region (PONDR) is a computer program that predicts whether any region of a peptide with a given sequence is disordered or not. By using it, I found that Subregions I and V are probably disordered (Fig. 6A). It should be noted that this finding is highly consistent with wet experiments shown in Kimata *et al.* (2004) and Oikawa, *et al*. (2005). This experiment suggests that Subregion I and V are high protease accessibility by proteolytic analysis. On the contrary, the PONDR predicts that the CSSR is folded, which is also consisted with the X-ray crystal structure of this region (Credle, *et al.*, 2005).

Metazoan PERK carries a luminal region which carries structural homology with Ire1 (Korennykn & Walter, 2012). I think that the luminal domains of PERK and Ire1 share the same or similar function, since a chimeric mutant of yeast Ire1 carrying the PERK luminal domain worked to sense ER stress and to evoke the UPR in yeast cells (Lui, *et al.*, 2000). While the amino-acid sequences of the PERK CSSR and that of Ire1 are highly conserved, the N-terminal region of PERK, which is approximately 80 a.a. long, has no sequence similarity with Subregion I of yeast Ire1. The PONDR program predicted that the N-terminal regions of mouse and human PERK, as well as that of the fungal Ire1 orthologue from *Aspergillus oryzae*, are highly disordered (Fig.

6B). Although no sequence similarity was observed, I think that the N-terminal region of PERK may correspond to Subregion I of yeast Ire1, since in general, amino-acid sequence of a natively disordered region is evolutionally less conserved even if it keeps a conserved function.

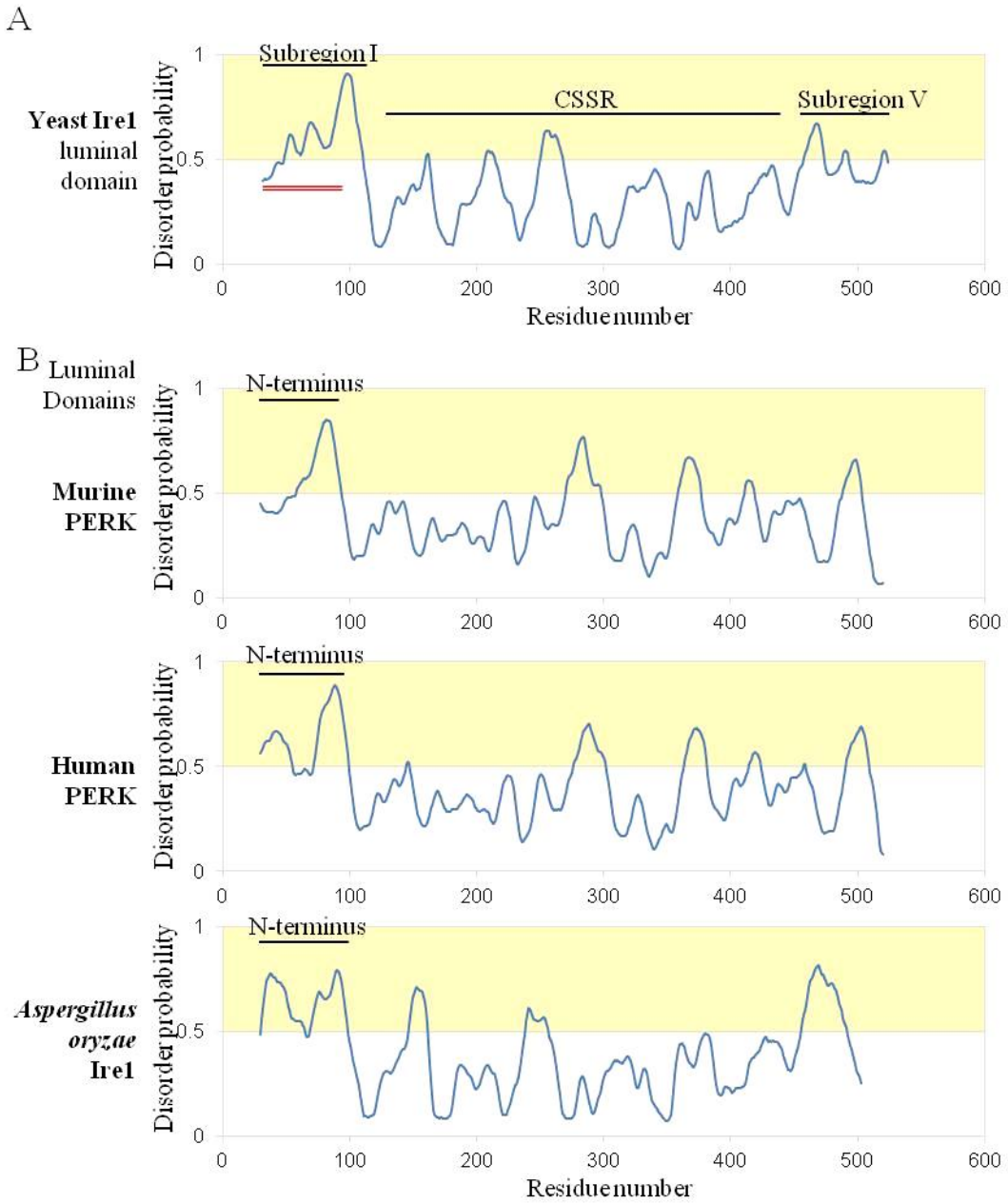

Figure 6. Disorder prediction of yeast Ire1 and its family proteins. Yeast Ire1 luminal domain (A) and human PERK, mouse PERK and *Aspergilus oryzae* Ire1 luminal domains (B) were analyzed by the PONDR program. The yellow-colored region means that the peptide is probably disordered.

3.2 A function of Subregion I to suppress activity of yeast Ire1 under non-stress conditions

In order to elucidate how Subregion I affects activity of Ire1, I used a reporter system named as the UPRE-*lac*Z reporter, in which β-galactosidase was expressed under the control of the UPR-target promoter element (Mori, *et al.*, 1992). As shown in Fig. 5A, I generated partial deletion mutations of yeast Ire1. The deletion of the anterior 60 a.a. of Subregion I was named as the ΔI mutation (Oikawa *et al.*, 2007). Because ΔI Ire1 carries the three-fourths portion of Subregion I, I also generated the deletion of the full-length 80-a.a. Subregion I, which I named as ΔI_{full}. The deletion of the posterior 20 a.a. of Subregion I was named as $\Delta I_{posterior}$. The ΔV mutation means a full-length deletion of Subregion V.

Through the UPRE-*lac*Z reporter assay shown in the left panel of Fig. 7A, I estimated UPR-inducing activity of the Ire1 mutants in non-stressed cells. The results indicate that the ΔV single mutant version of Ire1 exhibited slightly higher activity than wild-type Ire1 in non-stressed cells. On the contrary, none of the Subregion I-deletion mutations seemed to obviously activate wild-type Ire1. Reproducing a previous report by Oikawa *et al*. (2007), ΔV Ire1 exhibited a more potent activity in non-stressed cells when it is combined with the ΔI mutation (ΔIΔV Ire1). This finding implies that Subregions I and V additively and complementally function to suppress Ire1's activity. Activity of $\Delta I_{posterior}\Delta V$ Ire1 was not different from that of ΔV Ire1, suggesting that the posterior 20 a.a. of Subregion I has no important role in regulation of Ire1. Meanwhile, activity of $\Delta I_{full}\Delta V$ Ire1 was lower than that of ΔIΔV Ire1. I thus think that protein integrity of Ire1 may be somehow damaged by the ΔI_{full} mutation partially, and employed the ΔI mutation but not the ΔI_{full} mutation to explore a role of Subregion I to suppress Ire1's activity throughout the present study. Fig. S1 shows anti-HA Western-blot detection of Ire1-HA form cell lysates, which indicates that neither the ΔI mutation nor the ΔV mutation impaired cellular expression level of Ire1.

All of the Ire1 mutations employed here well responded to treatment of cells with tunicamycin, which is an N-glycosylation inhibitor and causes potent ER stress (Fig. 7A, right panel). In other words, even with the ΔIΔV mutation, Ire1 undergoes another regulation for full activation upon ER stress. Kimata *et al.* (2007) previously argued

that ΔIΔV Ire1 is constitutively clustered, since anti-HA immunofluorescent staining of non-stressed cells showed a dot-like punctate distribution of the HA-tagged version of ΔIΔV Ire1 that was overexpressed from a 2μ multicopy plasmid (Signals from Ire1-HA that was expressed at an authentic level cannot be seen using anti-HA immunofluorescent-staining technique). In the present study, I asked if a similar observation is obtained when ΔIΔV Ire1 is expressed at an authentic level. I thus inserted the cDNA of a bright fluorescent protein mNeonGreen into the Ire1 gene, which was fused to a centromeric yeast plasmid vector for transformation of an *ire1Δ* strain. Figure 7B shows fluorescence microscopic images of the mNeonGreen-tagged versions of Ire1. As expected, wild-type mNeonGreen-Ire1 was diffusively distributed over the ER in non-stressed cells, whereas it exhibits dot-like distribution, which means the cluster formation of this protein, in response to treatment of cells with a potent ER stressor DTT. Intriguingly, the ΔIΔV mutant version of mNeonGreen-Ire1 showed a similar result as the wild-type version. In other words, unlike the previous report by Kimata *et al.* (2007), ΔIΔV Ire1 clustered not constitutively but dependently on ER stress. Thus cluster formation of Ire1 is regulated independently of Subregions I or V.

A

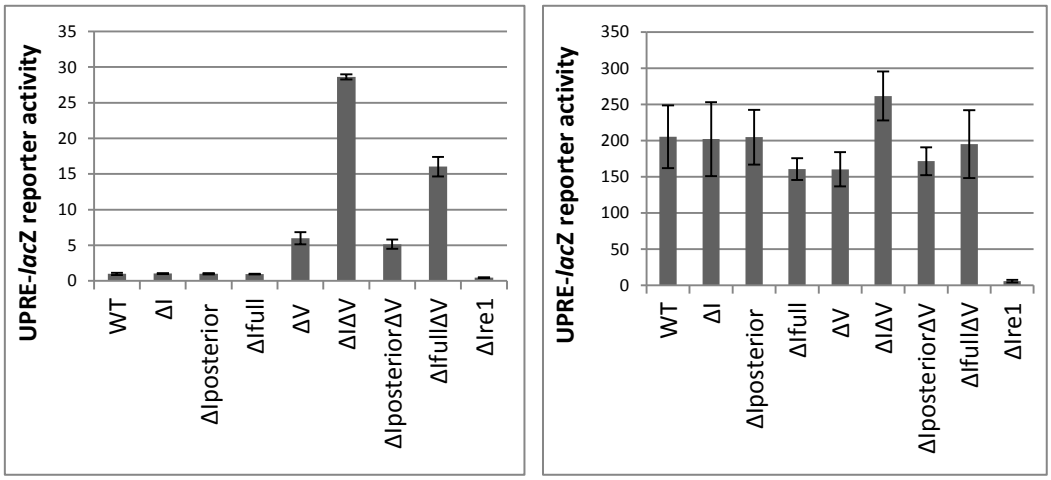

B

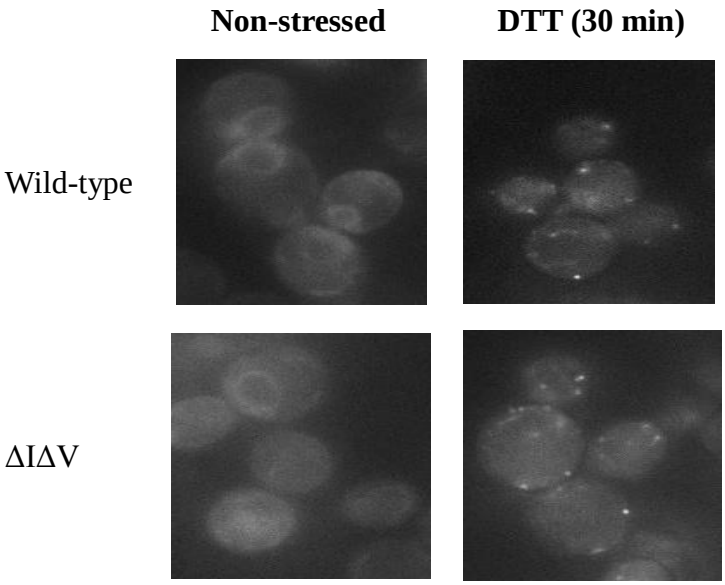

Figure 7. High activation of ΔIΔV Ire1 under non-stress conditions. (A) The Δ*ire1* strain KMY1015 containing the UPRE-*lac*Z reporter plasmid, pCZY1 and the *IRE1*-gene plasmid, which is derived from a yeast single-copy vector pRS313, or its *IRE1* mutants was assayed for cellular β-galactosidase assay. To induce ER stress, cells were treated with 2 μg/mL tunicamycin for 4 hr. (B) The Δ*ire1* strain KMY1015 containing the pRS313 vector fused with the mNeonGreen-inserted version of the *IRE1* gene or its ΔIΔV mutant was observed under the fluorescence microscope. To induce ER stress, cells were treated with 10 mM DTT for 30 min.

3.3 Activation of Ire1 by the ΔI Ire1 single mutation was observable through monitoring the *HAC*1-mRNA splicing.

We next monitored cellular activity of Ire1 through another methodology, which is to observe *HAC*1 mRNA splicing, since *HAC*1 mRNA is a direct target of yeast Ire1. As performed in Promlek *et al.* (2011), *HAC*1 mRNA spieces were amplified from total RNA samples using the reverse transcriptase-PCR technique, and the portion of *HAC*1^{i} mRNA in total *HAC*1 mRNA species (*HAC*1^{i} mRNA plus *HAC*1^{u} mRNA) was calculated and expressed in Figure 8 as "*HAC*1 mRNA splicing (%)".

As shown in Figure 8A, under non-stress or weak stress (0.5 mM DTT) conditions, ΔI Ire1 exhibited higher level of *HAC*1 mRNA splicing than wild-type Ire1, while strong ER stress (3 or 10 mM DTT) induced *HAC*1 mRNA splicing equally by wild-type Ire1 and ΔI Ire1. In other words, activation of Ire1 by the ΔI single mutation was observable not by the UPRE-lacZ reporter assay but by the monitoring *HAC*1 mRNA splicing, suggesting that results from these two methodologies are not linearly correlated. ΔV Ire1 and ΔIΔV Ire1 also exhibited activities higher than wild-type Ire1 under no or weak ER-stress conditions, and were fully activated by stronger ER stress.

As shown in Figure 8B, during a time-course induction by 3 mM DTT, wild-type, ΔI, and ΔV Ire1 reached a maximun level of *HAC*1 mRNA splicing quickly and equally, while wild-type Ire1 exhibited faster attenuation of activity than ΔI Ire1 and ΔV Ire1. In other words, the ΔI mutation slightly prolonged *HAC*1 mRNA splicing (Fig. 8B; 2hr-4hr), and such a retardation of activity attenuation upon long-term ER stress was more obvious in the case of the ΔV mutation.

A

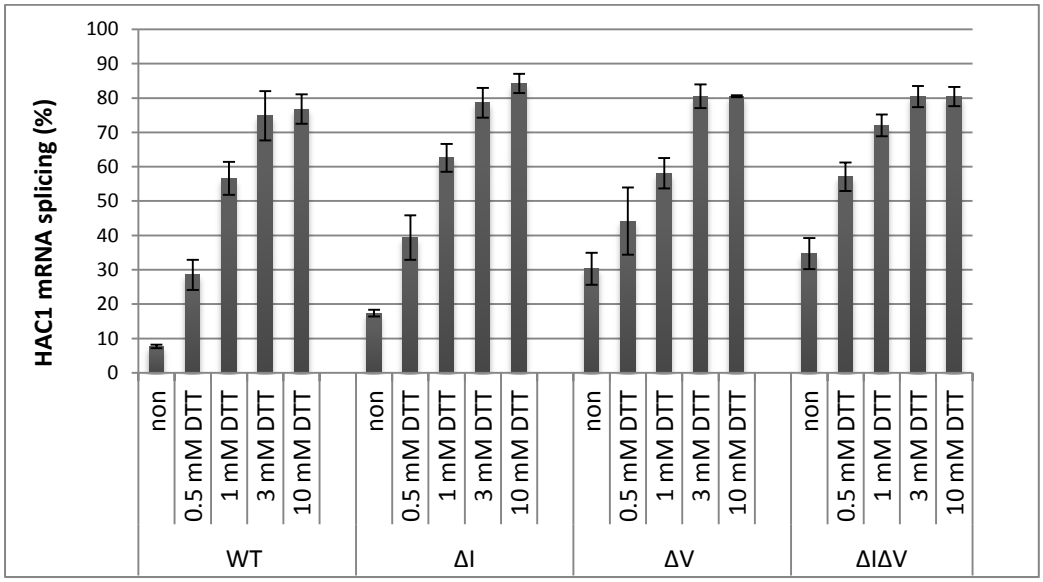

B

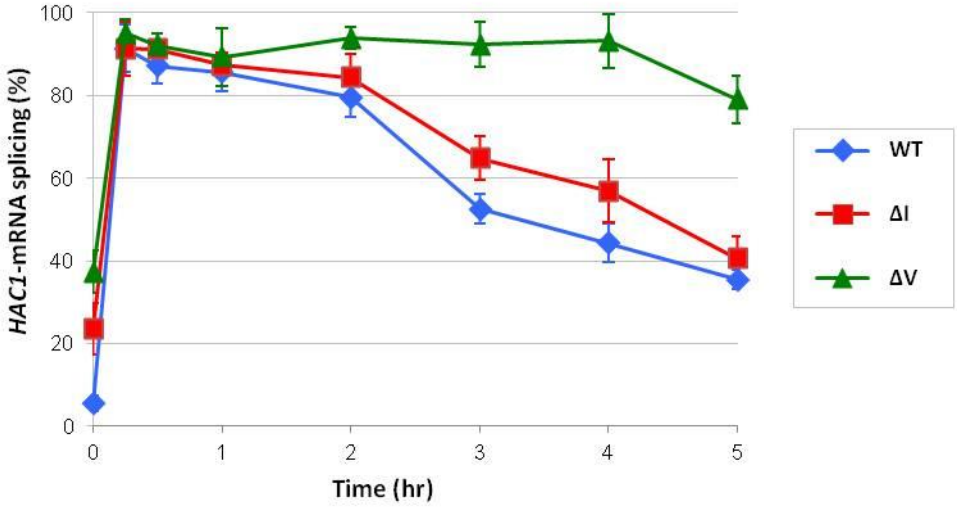

Figure 8. *HAC*1 mRNA splicing by wild-type Ire1 and its mutants. The Δ*ire1* strain KMY1516 transformed with the single-copy plasmid vector pRS313 containing the *IRE*1 gene or its mutants was analyzed by RT-PCR of the total RNA samples to evaluate splicing efficiency of *HAC*1 mRNA. (A) Cells were stressed by DTT at the indicated concentrations for 30 min. (B) Cells were stressed by 3 mM DTT for the indicated durations.

3.4 Primary-structural requirement of Subregion I for its ability to suppress Ire1's activity

The UPRE-lac*Z* reporter values of ΔV-*IRE*1 and ΔIΔV-*IRE*1 cells under non-stressed conditions were considerably different (Fig. 7A), allowing us to perform quick and high-resolution monitoring of the Ire1-suppressing ability of Subregion I and its mutants. Thus, we modified ΔV Ire1 by introducing various mutations into its Subregion I and tested for its activity to induce the UPRE-lacZ reporter in non-stressed cells, in order to address the primary structural requirements of Subregion I for its Ire1-suppressing ability.

As shown in Figure 5, the 80 a.a.-long Subregion I was divided into eight 10 a.a.-long segments, namely Segment 1 to 8. Figure 5B illustrates serial deletion mutations of these segments that were introduced into ΔV Ire1. UPR activity in non-stressed ΔV-*IRE*1 cells were modestly enhanced when the Δ1-4, Δ3-6, Δ4-6, Δ3-4 orΔ4 mutation was introduced, indicating that the ability of Subregion I to suppress Ire1's activity is partially compromised by these mutations, which commonly lack Segment 4 (Fig. 9A). In contrast, the other mutants in which Segment 4 was not deleted did not significantly alter the activity of ΔV Ire1 (Fig. 9A). These observations suggest an importance of Segment 4 for the Ire1-suppressing ability of Subregion I, whereas Subregion I not carrying Segment 4 worked only weakly.

We next confirmed the high Ire1-suppressing ability of Segment 4 through substituting three tandem repeats of Segment 4 on the first 60-a.a. portion of Subregion I (Segments 1-6) of ΔV Ire1 ($(Segment4)_3$ΔV Ire1). As shown in Figure 9C, the $(Segment\ 4)_3$ mutation drastically diminished the activity of ΔV Ire1 in non-stressed cells. On the other hand, an artificial disordered peptide, six tandem repeats of Gly-Gly-Gly-Ser-Ser ($(GGGSS)_6$ΔV), showed an weak Ire1-suppressing ability when substituted on Subregion I.

Because all mutants responded well to ER stress induced by tunicamycin (Fig. 9B and D) and did not seem to show impairment in their expression level (Fig. S1), I think that these mutations do not damage stability and function of Ire1.

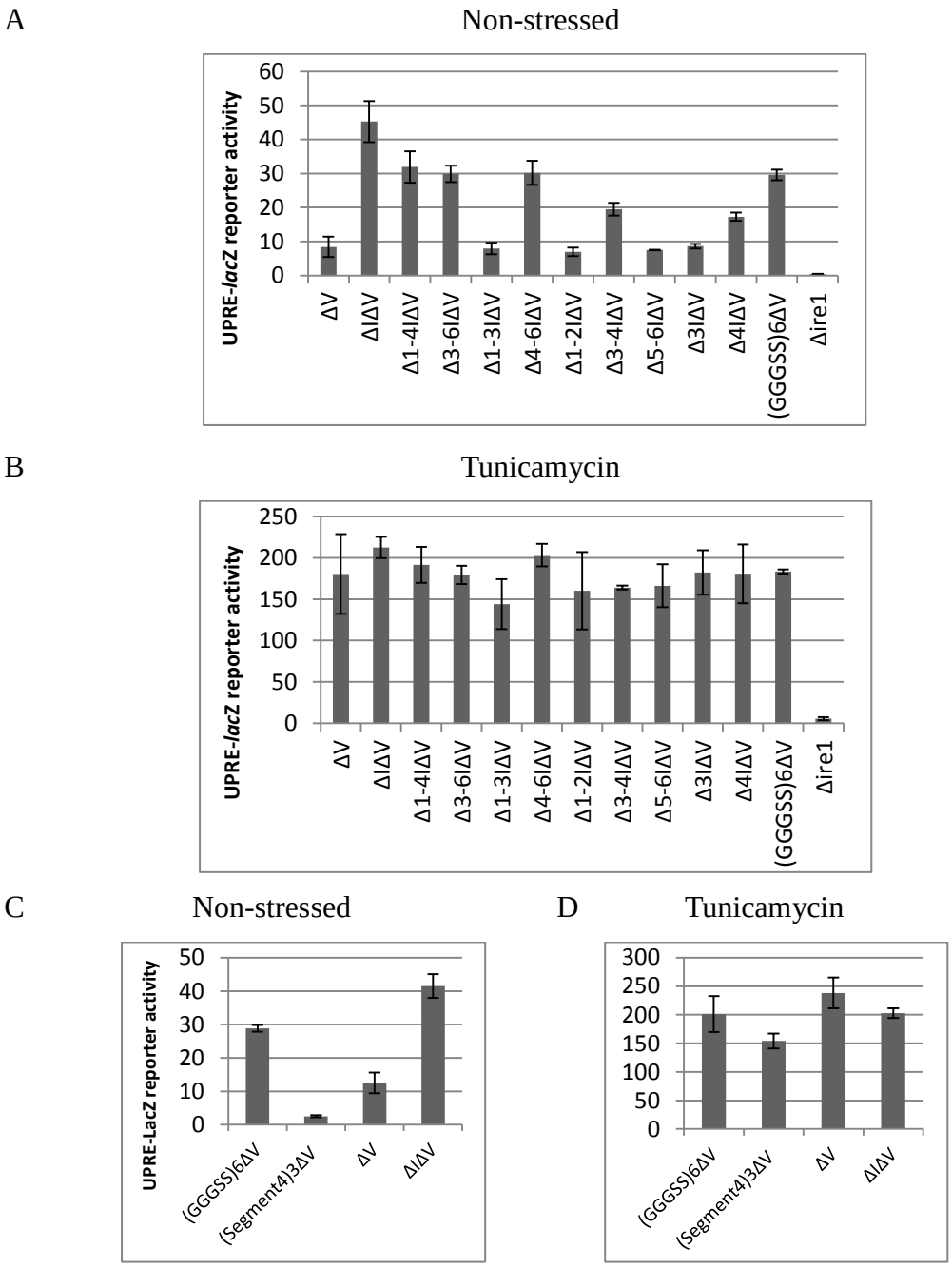

Figure 9. Activity of Ire1 carryig Subregion-I mutants. The Δ*ire1* strain KMY1015 containing the UPRE-*lac*Z reporter plasmid pCZY1 and single-copy plasmid vector pRS313 fused with the *IRE1* gene carrying the indicated mutations (see Fig. 5B and C) were assayed for cellular β-galactosidase activity. In the experiments shown in panels B and D, cells were stressed by 2 μg/mL tunicamycin for 4 h before the β-galactosidase assay.

3.5 Function of the N-terminal disordered regions of Ire1 orthologues and PERK is evolutionarily conserved

As touched on Figure 5B, metazoan PERK is predicted to have a disordered region, which probably functions as Subregion I, at its N terminus. In order to test if this region actually works as Subregion I, I constructed yeast Ire1 chimeric mutants in which 56-a.a.-long N-terminal disordered regions of human and mouse PERK were substituted on Subregion I (Segments 1-6) of yeast ΔV Ire1 (Fig. 5C; hPERKΔV and mPERKΔV Ire1) and checked their activity through the UPRE-*lac*Z reporter assay. In addition, the N-terminal disordered sequence of *Aspergillus oryzae* Ire1, which corresponds to Subregion I, was also used in this experiment (AIre1ΔV Ire1).

As shown in Figure 10A, activity of hPERKΔV, mPERKΔV Ire1 and AIre1ΔV Ire1 was lower than that of ΔV Ire1, which carries the authentic Subregion I of yeast Ire1, in non-stressed cells. I thus think that the N-terminal disorder regions of PERK and *Aspergillus oryzae* Ire1 work strongly as Subregion I to suppress Ire1's activity.

Because all mutants responded well to ER stress induced by tunicamycin (Fig. 10B) and did not seem to show impairment in their expression level (Fig. S1), I think that these mutations do not damage stability and function of Ire1.

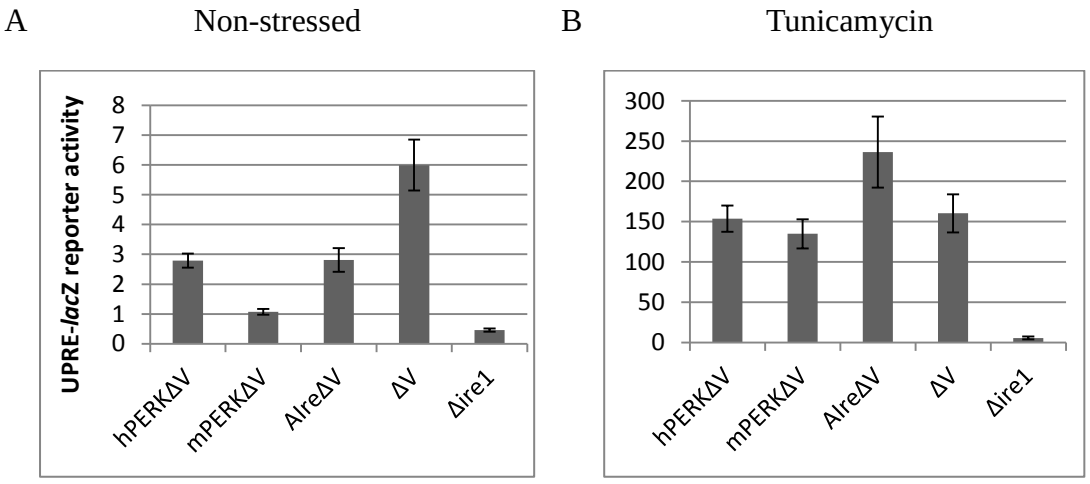

Figure 10. Suppression of yeast Ire1's activity by the N-terminal disordered region of PERK and fungus Ire1. The Δ*ire1* strain KMY1015 containing the UPRE-*lac*Z reporter plasmid pCZY1 and single-copy plasmid vector pRS313 fused with the *IRE1* gene carrying the indicated mutations (see Fig. 5C) were assayed for cellular β-galactosidase activity. In the experiments shown in panel B, cells were stressed by 2 μg/mL tunicamycin for 4 h before the β-galactosidase assay.

3.6 Physical interaction of Subregion I with the CSSR

In the experiment shown Figure 11A, disordered regions of non-related proteins, San1 and TOPII (two tandem copies; $(TOPII)_2$) (Berger, *et al.*, 1996; Rosenbaum, *et al.*, 2011), were substituted on Subregion I of ΔV Ire1 (Fig. 5C), and the resulting mutants were checked for activity to induce the UPRE-*lac*Z reporter in non-stressed cells. The disordered fragment from San1 exhibited a Subregion I-like Ire1-suppressing ability, which is only weak in the case of the disordered fragment from TOPII.

As a possible mechanism by which Suregion I suppresses Ire1's activity, I hypothesized that Subregion I might be captured by the CSSR as a unfolded-protein substrate. This is because various disordered peptides act as Subregion I to suppress Ire1's activity and because the CSSR is thought to capture various unfolded proteins. I thus performed experiments using a yeast two-hybrid system to check interaction of various peptides with the CSSR protein.

In Figure 11B, row 1, a positive interaction of the first 60-a.a. portion of Subregion I with the CSSR was observed. In contrast, such a two-hybrid interaction was not observed when the CSSR carried the ΔIII or the MFY mutation (Fig. 11A, rows 2 and 3), which impairs the ability of the CSSR to capture unfolded proteins. This finding indicates that Subregion I is actually captured by the CSSR as an unfolded-protein substrate.

In the experiment shown in Figure 11C (and Fig. S3 for the negative control), I observed two-hybrid interactions of the CSSR with various peptides which according to my data presented in Figure 9, 10 and 11A, showed strong or weak Ire1-suppressing activity when substituted on Subregion I of ΔV Ire1. Notably, the peptides which showed two-hybrid interaction to the CSSR only weakly (tandem repeats of GGGSS, Segments 1 to 3 and the disordered sequence from San1; Fig. 11C, rows 3, 4 and 8), namely slow growth on the two-hybrid agar plate, commonly exhibited only weak ability to suppress Ire1 when substituted on Subregion I (Fig. 9, 10 and 11A). In other words, abilities of a peptide to be captured by the CSSR and to suppress Ire1's activity as Subregion I are positively correlated.

A

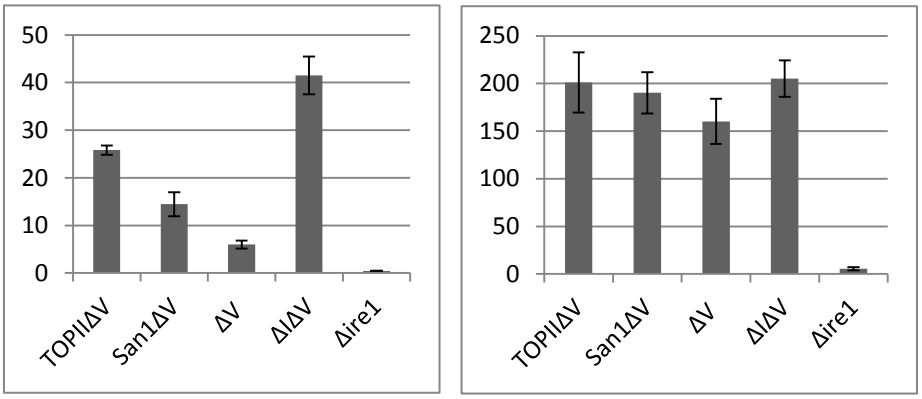
Non-stressed
Tunicamycin
50
40
30
20
10
0
250
200
150
100
50
0
TOPIIΔV
San1ΔV
ΔV
ΔIΔV
Δire1

B

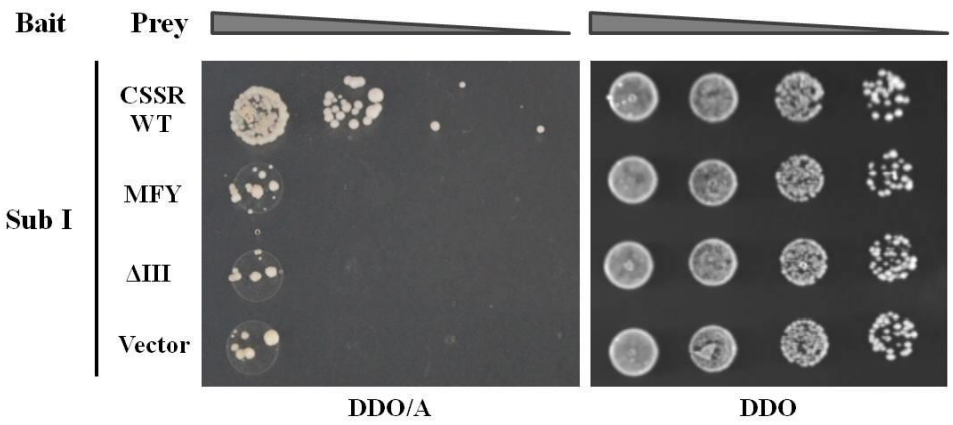
Bait
Prey
Sub I
CSSR WT
MFY
ΔIII
Vector
DDO/A
DDO

C

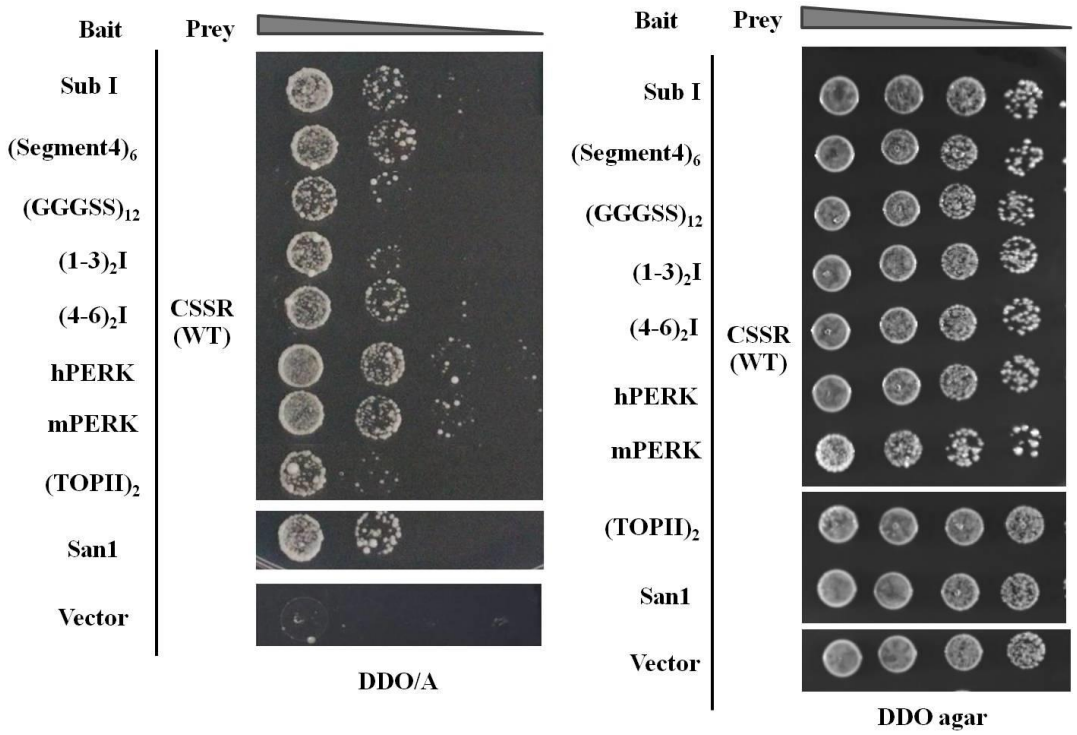

Figure 11. Subregion I is captured by the CSSR. (A) The Δ*ire1* strain KMY1015 containing the UPRE-*lac*Z reporter plasmid pCZY1 and single-copy plasmid vector pRS313 fused with the *IRE1* gene carrying the indicated mutations (see Fig. 5C) were assayed for cellular β-galactosidase activity. In the experiments shown in the right panel, cells were stressed by 2 μg/mL tunicamycin for 4 h before the β-galactosidase assay. (B and C) A yeast two-hybrid analysis was performed using the CSSR and its mutants as prey. The Subregion-I 60-a.a. portion (Sub I), Segment 4 (six tandem repeats), GGGSS (12 tandem repeats), Segments 1–3 (1–3; a.a. 32–61 of yeast Ire1; two tandem repeats), Segments 4–6 (4–6; a.a. 62–91 of yeast Ire1; two tandem repeats), the N-terminal disordered region of human or mouse PERK (hPERK or mPERK), the TOPII disordered region (TOPII; two tandem repeats) and the San1 disordered region (San1) were used as baits. Tester cell cultures were serially diluted 10-fold, spotted on agar plates, incubated for 2–4 days, and photographed. The two-hybrid tester cells grow on the DDO/A agar plates when the two-hybrid interaction is positive. The DDO agar plates serve as growth control.

3.7 Tight association of Segment 4 with the CSSR

My results shown in Figure 9 indicate that among the eight segments of Subregion I, Segment 4 is most important for the Subregion-I's ability to suppress activity of Ire1. I thus think that Sugment 4 may be captured by the CSSR more strongly than the other segments. I thus checked *in vitro* affinity of each Segment to the CSSR using chemically synthesized peptides listed on Table 1.

ΔEspP is a signal peptide carrying many hydrophobic and basic amino-acid residues to be a high-affinity substrate of the CSSR (Gardner & Walter, 2011). Therefore, according to Gardner & Walter (2011), fluorescence anisotropy of fluorescently labeled ΔEspP, namely the ΔEspP-FAM, in a solution is increased when it is mixed with a CSSR protein. In my experiment, the CSSR protein was expressed from *E. coli* and purified as described previously (Kimata, *et al.*, 2007). I then confirmed increment of ΔEspP-FAM's fluorescence anisotropy by addition of the purified CSSR protein (Fig. S2).

In the experiment shown in Figure 12, I performed a competitive interaction assay using a mixture of fixed concentrations of ΔEspP-FAM and the CSSR protein, into which a peptide corresponding to Segment 2, 3, 4, 5 or 6 was added at various concentrations. As expected, I then found that the Segment-4 peptide caused a reduction of ΔEspP-FAM's fluorescence anisotropy, in other words dissociation of ΔEspP-FAM from the CSSR protein, more efficiently than the other peptide corresponding to the other peptides.

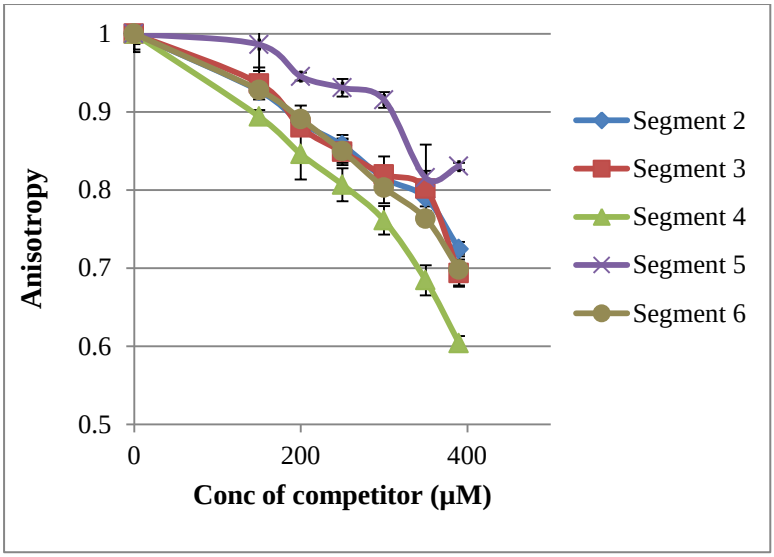

Figure 12. *In vitro* competition between ΔEspP-FAM and Subregion-I Segment peptides for association with the CSSR protein. A competitor peptide, which corresponds to one of the Segments of Subregion I, was added at various concentrations into a mixture of 10 µM ΔEspP-FAM and 5 µM of the purified CSSR protein, which was then incubated at room temperature for 45 min and subjected to a single tube Beacon2000 for measuring fluorescence polarization signal.

3.8 Self-association of the CSSR is compromised by its intramolecular interaction to Subregion I

My findings presented so far led me to presume a molecular model for the function of Subregion I, which may be intramolecularly captured by the CSSR and inhibit its homo-association to suppress Ire1's activity as illustrated in Figure 13A. In the experiment shown in Figure 13B, I monitored homo-association of the CSSR using the yeast two-hybrid system. In other words, the CSSR sequence was used both as the bait and the prey in the two-hybrid assay. The second row of Figure 13B shows a positive two-hybrid interaction between two CSSR proteins. As for the uppermost row of Figure 13B, the bait CSSR protein carried Subregion I and named as I-CSSR, which in other words, was composed of Subregions I to IV. Importantly, the bait I-CCSR failed to show two-hybrid interaction to the prey CSSR. However, when the bait I-CSSR carries the ΔIII or the MFY mutation, which impairs capturing of unfolded-protein substrate by the CSSR cavity, it interacted to the prey CSSR (row 3 and 4, Fig. 13B). These findings are consistent with my hypothesis in which Subregion I is intramolecularly captured by the substrate (unfolded protein)-binding cavity of the CSSR to inhibit homo-association of the CSSR.

In conclusion, this report has elucidated the undiscovered function of Subregion I. Under non-stress condition, Subregion I facilitated a negative regulation of Ire1 together with BiP association with Subregion V. Here I propose that this is caused by intramolecular capturing of Subregion I by the CSSR, which inhibits homo-association of Ire1.

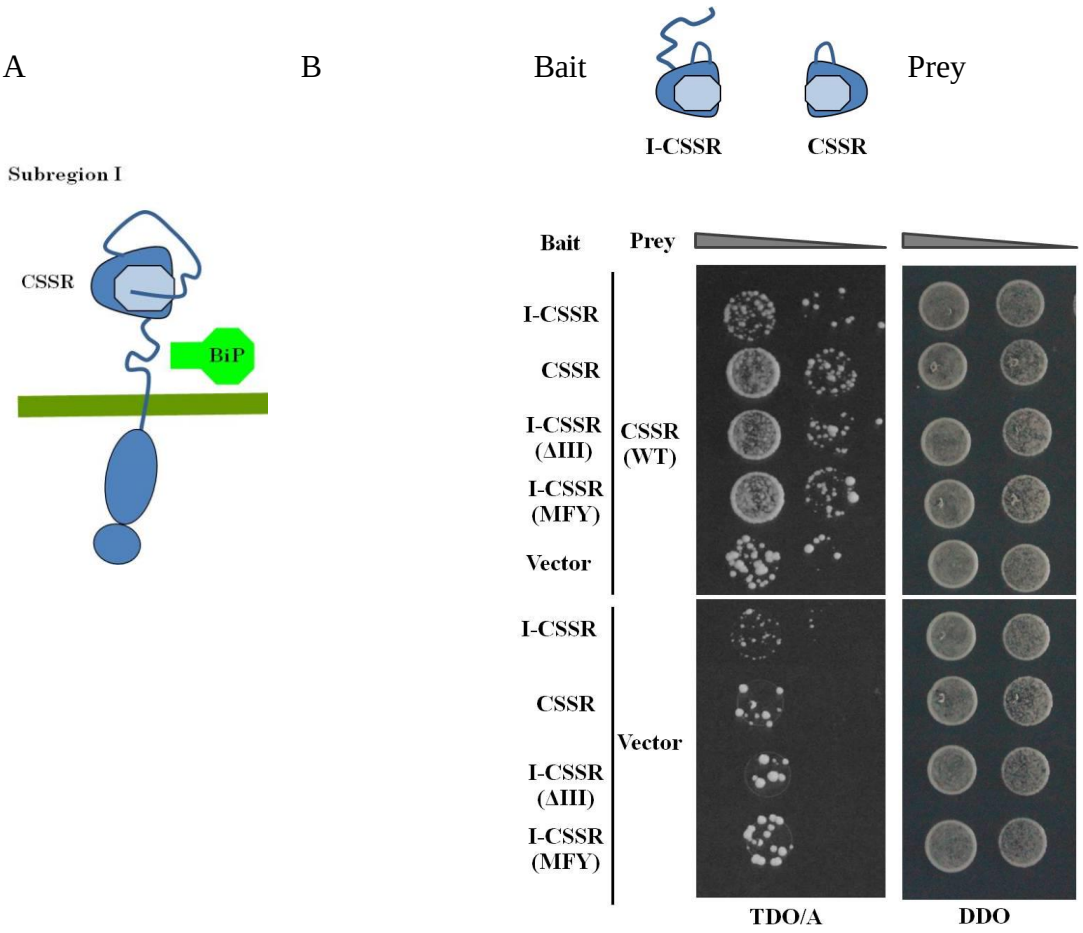

Figure 13. Intramolecular binding of Subregion I to CSSR domain. (A) The model structure of Ire1 under non-stress conditions. In this model Subregion I is captured by the CSSR. (B) A yeast two-hybrid analysis was performed using the CSSR and its derivative both as bait and prey. Tester cell cultures were serially diluted 10-fold, spotted on agar plates, incubated for 2–4 days, and photographed. The two-hybrid tester cells grow on the TDO/A agar plates when the two-hybrid interaction is positive. The DDO agar plates serve as growth control.

CHAPTER IV
DISCUSSION

A number of recent studies on structure and function of yeast Ire1 have provided insights into the molecular mechanism by which Ire1 responds to accumulation of unfolded proteins in the ER lumen and activates the downstream signal through the UPR pathway. Kimata *et al*., (2004) proposed that under non-stressed conditions, BiP, which is an Hsp70 family protein located in the ER lumen and plays a central role in maintaining protein quality control, is associated with the luminal domain of Ire1 and retains Ire1 in an inactive state until unfolded proteins are accumulated. In response to ER stress, BiP is rapidly dissociated from Ire1 probably because unfolded proteins are competitively bound to Ire1. However, dissociation of BiP from Ire1 is not sufficient for the full activation of Ire1 (Bertolotti, *et al.*, 2000; Oikawa, *et al.*, 2007). It is likely that the release of BiP from Ire1 produces free Ire1 molecules, which are homo-dimerized and then oligomerized (Credle, *et al.*, 2005; Kimata, *et al.*, 2007) through capturing unfolded proteins into the groove of the CSSR for full activation of Ire1 (Gardner & Walter, 2011; Promlek, *et al.*, 2011). The luminal domain of Ire1 can be divided into five Subregions, namely Subregion I to V from the N-terminus to the transmembrane domain (Kimata, *et al.*, 2004; Oikawa, *et al.*, 2007). Subregions II to IV compose the CSSR, and Subregion V serves as the BiP binding site. Meanwhile, roles of Subregion I, which is a loosely folded domain stretching out from the CSSR (Oikawa, *et al.*, 2005), have been poorly elucidated.

According to UPRE-lacZ reporter and *HAC1*-mRNA splicing assays using non-stressed yeast cells carrying *IRE1* mutations shown in this study (Fig. 7A and 8), Ire1 is slightly activated either by the ΔI or ΔV single mutation, whereas ΔIΔV Ire1 exhibited more potent activity. I thus think that Subregion I and the BiP-binding site, namely Subregion V, work as “double lock” to suppress Ire1’s activity in non-stressed cells. It is likely that Subregions I and V suppress not the cluster-formation step but a earlier step, probably dimer formation, of Ire1 activation, since ΔIΔV Ire1 as well as wild-type Ire1 clustered in response to ER stress (Fig. 7B). Remarkably, the function of Subregion I is independent of BiP, since wild-type Ire1 and ΔI Ire1equally exhibit

BiP association and dissociation dependently on ER stress (Oikawa, *et al.*, 2007). ER stress abolishes these suppressive events of Ire1, which is then clustered and fully activated by oligomer formation of the CSSR dependently on capturing unfolded proteins by the CSSR (Gardner & Walter, 2011).

Kawahara *et al*., (1997) reported that constitutive expression of the mature Hac1 protein caused severe growth retardation of yeast cells. Thus, the UPR must be properly tuned off to avoid hypersensitivity to small fluctuations in a normal condition. Consistently, according to a preliminary study in my research group, cells carrying the ΔI mutation on the *IRE1* gene exhibited slightly slower growth under non-stressed conditions than wild-type *IRE1* cells, suggesting a physiological importance of Subregion I on yeast cells.

What is the molecular mechanism of suppression of Ire1's activity by Subregion I? According to the yeast two-hybrid assays presented in this study, Subregion I acts as an intramolecular inhibitor of the interaction of two CSSR proteins (Fig. 13B), and a Subregion-I peptide physically interacts with the CSSR (Fig. 11A). I thus propose that Subregion I is intramolecularly captured by the CSSR to inhibit self-association of Ire1. It should be noted that Subregion I is natively disordered (Fig. 6A) and thus likely to be an unfolded-protein substrate of the CSSR groove. Although various disordered peptides suppressed Ire1's activity when substituted on Subregion I (Fig. 9 and 11A), Segment 4 is prominently important for the Ire1-suppressing activity of Subregion I and efficiently captured by the CSSR (Fig. 9A, 11B and 12). However, my point-mutation analysis of Segment 4 failed to determine amino-acid residues that are responsible for the Segment 4's function to suppress Ire1's activity.

Based on computational disorder prediction shown in Figure 6B, PERK and fungus Ire1 carry disordered regions on their N-terminus, and overall structure of their luminal domains seem to be evolutionarily conserved (Kimata, *et al.*, 2004). When substituted on Subregion I of yeast Ire1, the N-terminal disordered regions of PERK and fungus Ire1 strongly act to suppress Ire1's activity (Fig. 10). Since BiP is associated and dissociated from PERK as well as from Ire1 in response to ER stress (Bertolotti, *et al.*, 2000; Okamura, *et al.*, 2000), similarly to yeast Ire1, I think that PERK is dually suppressed by its N-terminal disordered region and BiP association. I speculate that tight suppression of PERK's activity is particularly important because it

induces reduction of general protein synthesis and cellular apoptosis, which highly damage cells (Harding, *et al.*, 1999; Wang, *et al.*, 1998; Zinszner, *et al.*, 1998). On the other hand, animal and plant Ire1 orthologues do not carry N-terminal disordered domains and thus are likely to be suppressed only by BiP association. I speculate that higher eukaryotic cells are quite sensitive to ER stress and thus the IRE1 orthologues have to be quickly activated even by weak ER stress. In other words, too tight repression of higher eukaryotic IRE1 orthologues may not be good for cells.

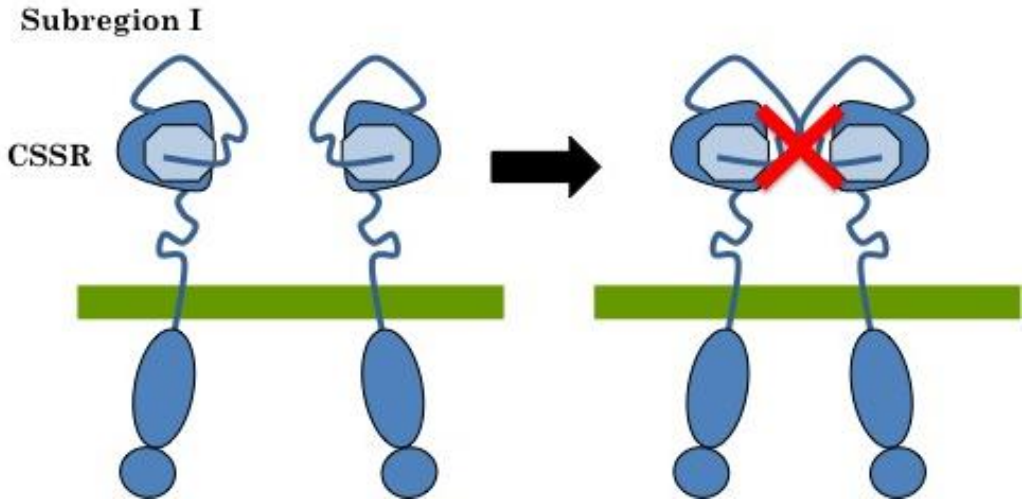

Figure 14. Model mechanism of Subregion I. Subregion I function as a negative regulator for Ire1 under nonstress condition. Subregion I is captured by the core stress sensing region (CSSR) and inhibit the dimerization or oligomerization, results to remain an inactive state of Ire1. When unfolded proteins accumulate in the ER lumen, this event causes the releasing of Subregion I from the CSSR. Unfolded proteins are captured groove domain of the CSSR and then fully activate Ire1.

ACKNOWNLEGDEMENTS

This research project would not have been possible without the support of many people. First, I would like to express my deepest and sincere gratitude to my advisor, Assoc Prof. Yukio Kimata for his meaningful supervision, kindness discussion, encouragement and personal guidance throughout my study.

My sincere appreciation is also grateful to Prof. Kenji Kohno for handing me a great opportunity to be a student in his laboratory and thank for his helpful comments and advices.

I would like to gratefully thank all of my advisory committees: Prof. Hiroshi Tagaki, and Prof. Kazuhiro Shiozaki, from Graduate School of Biological Science, NAIST for their valuable helpful suggestion and assistance throughout this research.

I appreciate Miss Tomoko Tsukamoto, graduated student, for being as nicely laboratory partner and her productively results. I am thankful to all members of Molecular and Cell Genetics Laboratory for their advices and supports. Special thank to Dr. Yuki Ishiwata-Kimata and Mr. Yuichi Tsuchiya, for their kindnesses, valuable comments, assistance and support during my study.

This work is supported by NAIST Global COE. I sincerely appreciate Graduate School of Biological Science, Nara Institute of Science and Technology, Japan, for providing research assistantship as well as for partial support for research work.

Finally, I would like to thank the support from my family and dear friends for their care and love.

Rubwad Mathuranyanon

REFERENCES

Aebi, M., Bernasconi, R., Clerc, S., & Molianri, M. (2010). N-glycan structures: recognition and processing in the ER. *Trends. Biochem. Sci, 35*, 74-82.

Aragon, T., Anken, V. E., Pincus, D., Serafimova, I. M., Korennykn, A., Rubio, C. A., *et al.* (2009). Messenger RNA targeting to endoplasmic reticulum stress signaling site. *Nature, 457*, 736-740.

Audesirk, T., & Audesirk, G. (1999). Biology, Life on Earth. . *Prentice Hall, 5th Edition*.

Berger, J. M., Gamblin, S. J., Harrison, S. C., & Wang, J. C. (1996). Structure and mechanism of DNA topoisomerase II. *Nature, 379*, 225-232.

Bertolotti, A., Zhang, Y., Hendershot, L. M., Harding, H. P., & Ron, D. (2000). Dynamic interaction of BiP and ER stress transducers in the unfolded-protein response. *Nat. Cell. Biol., 2*(6), 326-332.

Brodsky, J. L., & McCracken, A. A. (1999). ER protein quality control and proteasome-mediated protein degradation. *Semin. Cell Dev. Biol., 10*, 507-513.

Brodsky, J. L., & Skach, W. R. (2011). Protein folding and quality control in the endoplasmic reticulum: recent lessons from yeast and mammalian cell systems. *Curr. Opi. Cell. Biol., 23*, 464-475.

Celfon, M., Zeng, H., Urano, F., Till, J. H., Hubbard, S. R., Harding, H. P., *et al.* (2002). IRE1 couples endoplasmic reticulum load to secretory capacity by processing the XBP-1 mRNA. *Nature, 415*, 92-96.

Cox, J. S., & Walter, P. (1996). A novel mechnism for regulating activity of a transcription factor that controls the unfolded protein response. *Cell, 87*, 391-404.

Credle, J. J., Finer-Moore, J. S., Papa, F. R., Stroud, R. M., & Walter, P. (2005). On the mechnism of sensing unfolded protein in the endoplasmic reticulum. *Proc. Nati. Acad. Sci. USA., 102*, 18773-18784.

Cui, W., Li, J., Ron, D., & Sha, B. (2011). The structure of the PERK kinase domain suggests the mechanism for its activation. *Acta. Crystallogr. D., 67*(Pt 5), 423-428.

Ellgaard, L., & Helenius, A. (2003). Quality control in the endoplasmic reticulum. *Nature, 4*, 181-191.

Enger, E. D., & Ross, F. C. (2003). Concepts in Biology. *McGraw-Hill, 10th Edition*.

Folter, D. S., & Immink, R. G. H. (2011). Yeast protein-protein interaction assays and screens. *Methods in Molecular Biology, 754*, 145-165.

Gardner, B. M., Pincus, D., Gotthardt, K., Gallagher, C. M., & Walter, P. (2013). Endoplasmic reticulum stress sensing in the unfolded protein response. *Cold Spring Harb Perspect Biol., 5: a013169*.

Gardner, B. M., & Walter, P. (2011). Unfolded proteins are Ire1-activating ligands that directly induce the Unfolded Protein Respone. *Science, 333*, 1891-1894.

Glickman, M. H., & Ciechanover, A. (2002). The ubiquitin-proteasome proteolytic pathway: destruction for the sake of construction. *Physiol. Rev., 82*, 373-428.

Harding, H. P., Zhang, Y., & Ron, D. (1999). Protein translation and folding are coupled by an endoplasmic-reticulum-resident kinase. *Nature, 397*(6716), 271-274.

Harper, J. W., Adami, G. R., Wei, N., Keyomarsi, K., & Elledge, S. J. (1993). The p21 Cdk-interacting protein Cip1 is a potent inhibitor of G1 cyclin-dependent kinase. *Cell, 75*, 805-816.

Hendershot, L. M. (2004). The ER function BiP is a master regulator of ERfunction. *Mt. Sinai. J. Med., 71*, 289-297.

Hetz, C. (2012). The unfolded protein response: controlling cell fate decisions under ER stress and beyond. *Nat. Rev. Mol. Cell. Biol., 13*, 89-102.

Hetz, C., Martinon, F., Rodriquez, D., & Glimcher, L. H. (2011). The unfolded protein response: integrating stress signals through the stress sensor IRE1α. *Physiol. Rev., 91*, 1219-1243.

HO, S. N., Hunt, H. D., Horton, R. M., Pullen, J. K., & Pease, L. R. (1989). Site-directed mutagenesis by overlap extension using the polymerase chain reaction. *Gene., 77*, 51-59.

Hollien, J., & Weissman, J. S. (2006). Decay of endoplasmic reticulum-localized mRNAs duringh the unfolded protein response. *Science, 313*, 104-107.

Iwawaki, T., Akai, R., Yamanaka, S., & Kohno, K. (2009). Function of IRE1 alpha in the placenta is essential for placental development and embryonic viability. *Proc. Nati. Acad. Sci. USA., 106*(39), 16657-16662.

Iwawaki, T., Hosoda, A., Okuda, T., Kamigori, Y., Nomura, F. C., Kimata, Y., *et al.* (2001). Translational control by the ER transmembrane kinase/ribonuclease IRE1 under ER stress. *Nat. Cell. Biol., 3*(2), 158-164.

Kawahara, T., Yanagi, H., Yura, T., & Mori, K. (1997). Endoplasmic reticulum stress-induced mRNA splicing permits synthesis of transcription factor Hac1p/Ern4p that activates the unfolded protein response. *Mol. Biol. Cell, 8*, 1845-1862.

Kimata, Y., Ishiwata-Kimata, Y., Ito, T., Hirata, A., Suzuki, T., & Oikawa, D. (2007). Two regulatory steps of ER-stress sensor Ire1 involving its cluster formation and interaction with unfolded proteins. *J. Cell Biol, 179*, 75-86.

Kimata, Y., Kimata, Y. I., Shimizu, Y., Abe, H., Farcasanu, I. C., Takeuchi, M., *et al.* (2003). Genetic evidence for a role of BiP/Kar2 that regulates Ire1 in response to accumulation of unfolded proteins. *Mol. Biol. Cell, 14*, 2559-2569.

Kimata, Y., Oikawa, D., Shimizu, Y., Ishiwata-Kimata, Y., & Kohno, K. (2004). A role for BiP as an adjustor for the endoplasmic reticulum stress-sensing protein Ire1. *J. Cell Biol., 167*, 445-456.

Kohno, K. (2010). Stress-sensing mechanisms in the unfolded protein: similarities and differences between yeast and mammals. *J. Biochem., 147*(1), 27-33.

Korennykn, A., & Walter, P. (2012). Structural basis of the Unfolded Protein Response. *Annu. Rev. Cell Dev. Biol., 28*, 251-277.

Lui, C. Y., Schroder, M., & Kaufman, R. J. (2000). Ligand-independent dimerization activates the stress response kinases IRE1 and PERK in the lumen of the endoplasmic reticulum. *J. Biol. Chem, 275*(32), 24881-24885.

Ma, K., Vattem, K. M., & Wek, R. C. (2002). Dimerization and release of molecular chaperone inhibition facilitate activation of eukaryotic initiation factor-2 kinase in response to endoplasmic reticulum stress. *J. Biol. Chem, 277*, 18728-18735.

Malhotra, J. D., & Kaufman, R. J. (2007). The endoplasmic reticulum and the unfolded protein response. *Semin. Cell Dev. Biol., 18*, 716-731.

Mori, K. (2003). Frame switch splicing and regulated intramembrane proteolysis: key words to understand the unfolded protein response. *Traffic, 4*, 519-528.

Mori, K. (2009). Signalling pathways in the unfolded protein response: Development from yeast to mammals. *J. Biol. Chem, 146*, 743-750.

Mori, K., Sant, A., Kohno, K., Normington, K., Gething, M. J., & Sambrook, J. F. (1992). A 22 bp cis-acting element is nescessary and sufficient for the induction of yeast KAR2 (BiP) gene by unfolded proteins. *EMBO J., 11*, 2583-2593.

Muhlrad, D., Hunter, R., & Parker, R. (1992). A rapid method for localized mutagenesis of yeast genes. *Yeast, 8*, 79-82.

Oikawa, D., Kimata, Y., & Kohno, K. (2007). Self-association and BiP dissociation are not sufficient for activation of the ER stress sensor Ire1. *J. Cell. Sci., 120*(9), 1681-1688.

Oikawa, D., Kimata, Y., Takeuchi, M., & Kohno, K. (2005). An essential dimer-forming subregion of the endoplasmic reticulum stress sensor Ire1. *Biochem. J., 391*, 135-142.

Okada, T., Haze, K., Nadanaka, S., Yoshida, H., Seidah, N. G., Hirano, Y., *et al.* (2003). A serine protease inhibitor prevent endoplasmic reticulum stress induced cleavage but not transport of the menbrane-bound transcription factor ATF6. *J. Biol. Chem., 278*, 31024-31032.

Okamura, K., Kimata, Y., Higashio, H., Tsura, A., & Kohno, K. (2000). Dissociation of Kar2p/BiP from an ER senory molecule, Ire1p, triggers the unfolded protein response in yeast. . *Biochem. Biophys. Res. Commun., 279*, 445-450.

Otero, J. H., Lizak, B., & Hendershot, L. M. (2010). Life and death of a BiP substrate. *Semin. Cell Dev. Biol., 21*, 472-478.

Papa, F. R., Zhang, C., Shokat, K., & Walter, P. (2003). Bypassing a kinase activity with an ATP-competitive drug. *Science, 302*, 1533-1537.

Promlek, T., Kimata, I.-Y., Shido, M., Sakuramoto, M., Kohno, K., & Kimata, Y. (2011). Menbrane aberrancy and unfolded proteins activate the endoplasmic reticulum stress sensor Ire1 in different ways. *Mol. Biol. Cell, 22*, 3520-3532.

Romero, P., Obradovic, Z., Li, X., Garner, E. C., Brown, C. J., & Dunker, A. K. (2001). Sequence complexity of disordered protein. *Proteins, 42*, 38-48.

Ron, D., & Walter, P. (2007). Siganl inegration in the endoplasmic reticulum unfolded protein response. *Nat. Rev. Mol. Cell. Biol., 8*, 519-529.

Rosenbaum, J. C., Fredrickson, E. K., Oeser, M. L., Garrett-Engele, C. M., Locke, M. N., Richardson, L. A., *et al.* (2011). Disorder targets misorder in nuclear quality control degradation: a disordered ubiquitin ligase directly recognizeds its misfolded substrates. *Mol. Cell, 41*, 93-106.

Schroder, M., & Kaufman, R. J. (2005). The mammalian unfolded protein response. *Annu. Rev. Biochem., 74*, 739-789.

Shen, J., Chen, X., Hendershot, L. M., & Prywes, R. (2002). ER stress regulation of ATF6 localization by dissociation of BiP/GRP78 binding and unmasking of Golgi localization signals. *Dev. Cell., 3*, 99-111.

Sidrauski, C., & Walter, P. (1997). The transmembrane kinase Ire1p is a site-specifice endonuclease that initiates mRNA splicing in the unfolded protein response. *Cell, 90*, 1031-1039.

Sikorski, R. S., & Hieter, P. (1989). A system of shuttle vectors and yeast host strains designed for efficient manipulation of DNA in *Saccharomyces cerevisiae*. *Genetics, 122*, 19-27.

Tabas, I., & Ron, D. (2011). Integrating the mechanism of apoptosis induced by endoplasmic reticulum stress. *Nat. Cell. Biol., 13*(3), 184-190.

Taylor, R. C., & Dillin, A. (2013). XBP-1 is a cell-nonautonomous regulator of stress resistance and longevity. *Cell, 153*, 1435-1447.

Tirasophon, W., Welihinda, A. A., & Kaufman, R. J. (1998). A stress response pathway from the endoplasmic reticulum to the nucleus requires a novel bifunctional protein kinase/endoribonuclease (Ire1p) in mammalian cells. *Genes. Dev., 12*(12), 1812-1824.

Travers, K. J., Patill, C. K., Wodicka, L., Lockhart, D. J., Weissman, J. S., & Walter, P. (2000). Functional and genomic analyses reveal an essential coordination between the unfolded protein response and ER-associated degradation. *Cell, 101*, 249-258.

Tsai, Y. C., & Weissman, A. M. (2010). The unfolded protein response, degradation from the endoplasmic reticulum, and cancer. *Genes & Cancer., 1*(7), 761-778.

Tsuru, A., Fujimoto, N., Takahashi, S., Saito, M., Nakamura, D., Iwano, M., *et al.* (2013). Negative feedback by IRE1β optimizes mucin production in goblet cells. *Proc. Nati. Acad. Sci. USA., 110*(8), 2864-2869.

Vitale, A., Ceriotti, A., & Denecke, J. (1993). The role of the endoplasmic reticulum in protein synthesis, modification and intracellular transport. *J. Exp. Bot., 44*(9), 1417-1444.

Walter, P., & Ron, D. (2011). The unfolded protein response: from stress pathway to homeostasis regulation. *Science, 334*, 1081-1086.

Wang, X. Z., Kuroda, M., Sok, J., Batchvarova, N., Kimmel, R., Chung, P., *et al.* (1998). Identification of novel stress-induced genes downstream of chop. *EMBO J., 17*, 3619-3630.

Yani, C., & Federica, B. (2013). IRE1: ER stress sensor and cell fate executor. *Trend in Cell Biol., 23*(11), 547-555.

Ye, J., Rawson, R. B., Komuro., R., Chen, X., Dave, U. P., Prywes, R., *et al.* (2000). ER stress induces cleavage of membrane-bound ATF6 by the same proteases that process SREBOs. *Mol. Cell., 6*, 1355-1364.

Yoshida, H., Matsui, T., Yamamoto, A., Okada, T., & Mori, K. (2001). XBP1 mRNA is induced by ATF6 and spliced by IRE1 in response to ER stress to produce a highly active transcription factor. *Cell, 107*, 881-891.

Zinszner, H., Kuroda, M., Wang, X. Z., Batchvarova, N., Lightfoot , R. T., Remotti, H., *et al.* (1998). CHOP is implicated in programmed cell death in response to impaired function of the endoplasmic reticulum. *Genes. Dev., 12*, 982-995.

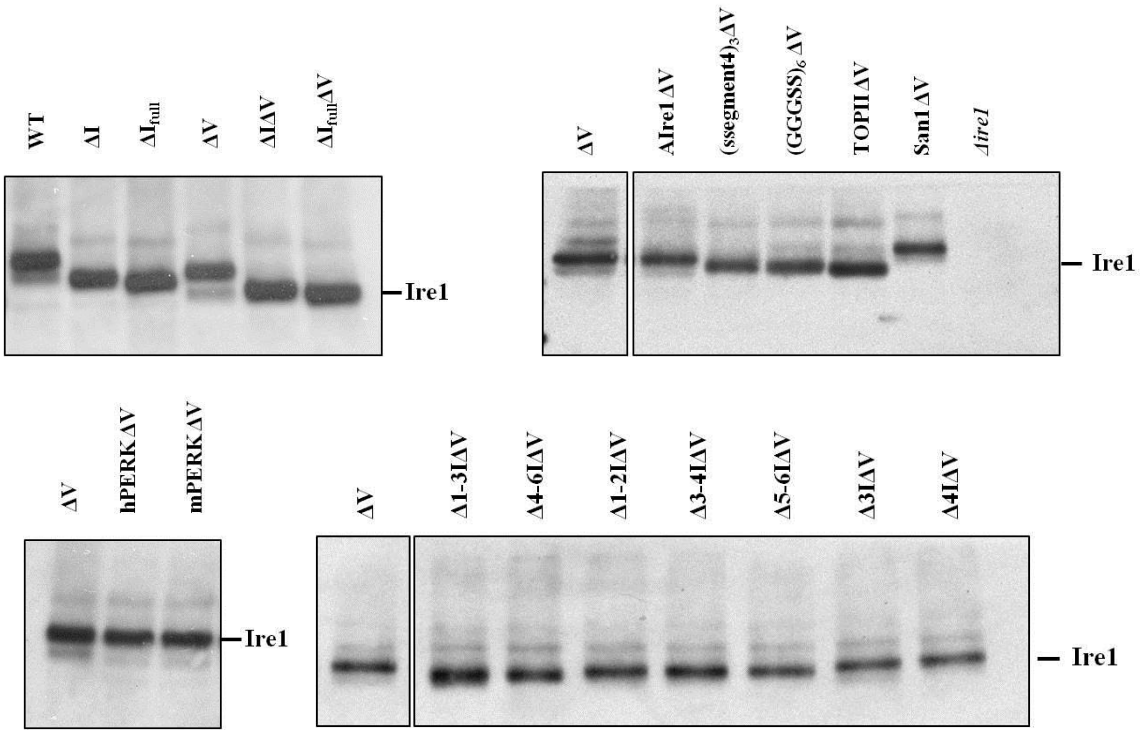

Figure S1. Cellular expression of wild-type and mutant Ire1. The C-terminally HA-epitope-tagged version of Ire1 (wild-type (WT)) and its mutants were expressed from the *IRE1* endogenous promoter in the KMY1015 (*Δire1*) strain using the single-copy plasmid vector pRS315. Total cell lysate samples were then used for anti-HA Western blot analysis.

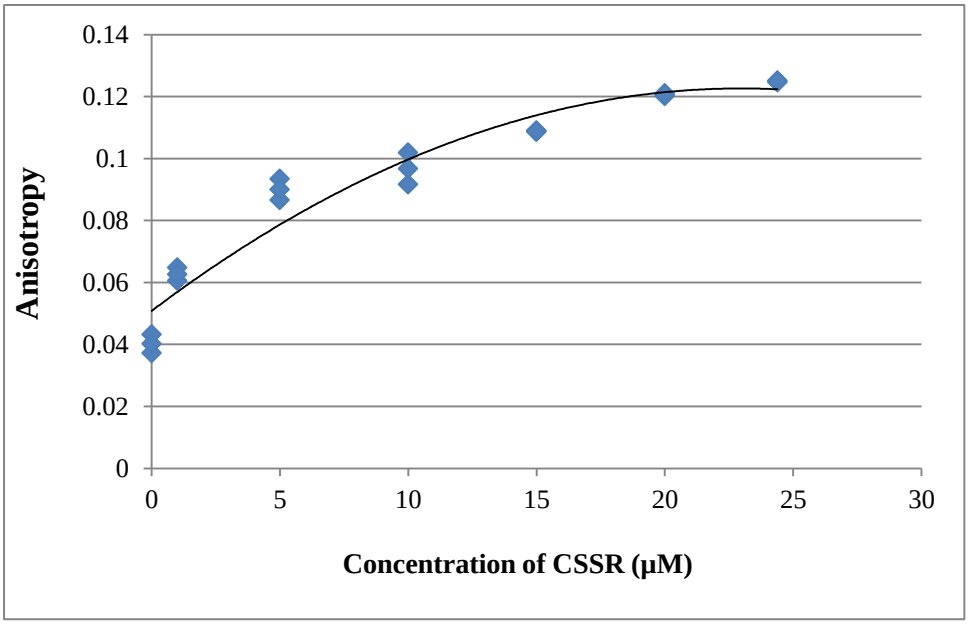

Figure S2. Fluorescence anisotropy of ΔEspP-FAM and its increment by the CSSR protein. ΔEspP-FAM (10 μM) was mixed with different concentrations of purified CSSR and incubated at room temperature for 30 min before measurement of fluorescence polarization. According to this figure, approximate K_D is estimated to be 2.5 μM.

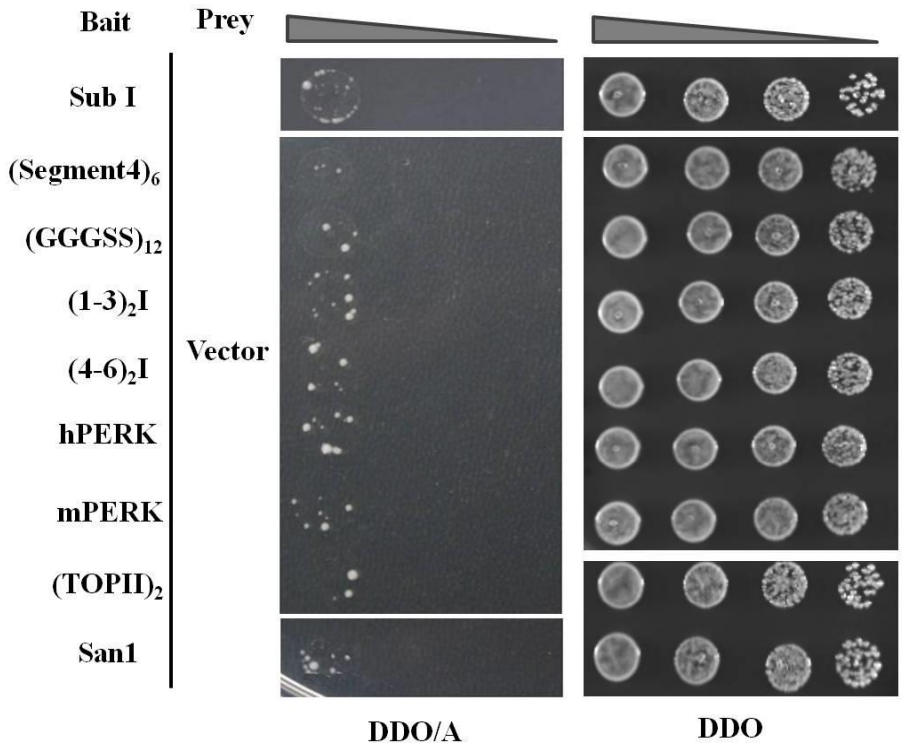

Figure S3. Negative control experiment for the yeast two-hybrid assay shown in Fig. 11C. The same experiment as Fig. 11C was performed using the empty-vector control as the prey.

List of Publications

Lab name (Supervisor)	Molecular and Cell Genetics (Ascco. Prof. Yukio Kimata)		
Name (surname) (given name)	Mathuranyanon Rubwad	Date	2014/11/19

Title: Tight regulation of the unfolded protein sensor Ire1 by its intramolecularly antagonizing subdomain

Authors: Rubwad Mathuranyanon, Tomoko Tsukamoto, Asumi Takeuchi, Yuichi Tsuchiya, Yuki Ishiwata-Kimata, Kenji Kohno, and Yukio Kimata

Year of issue: 2015

Name of Journal: Journal of Cell Science